NONEQUILIBRIUM DYNAMICS IN FIBER NETWORKS, AGGREGATION, AND SAND RIPPLES

Erkki Hellén

Laboratory of Physics
Helsinki University of Technology

Fysiikan laboratorio
Teknillinen korkeakoulu

DISSERTATION 116 (2002)

NONEQUILIBRIUM DYNAMICS IN FIBER NETWORKS, AGGREGATION, AND SAND RIPPLES

Erkki Hellén

Laboratory of Physics
Helsinki University of Technology
Espoo, Finland

Dissertation for the degree of Doctor of Science in Technology to be presented with due permission of the Department of Engineering Physics and Mathematics, Helsinki University of Technology for public examination and debate in Auditorium E at Helsinki University of Technology (Espoo, Finland) on the 8th of November, 2002, at 12 o'clock noon.

Dissertations of Laboratory of Physics, Helsinki University of Technology
ISSN 1455-1802

Dissertation 116 (2002):
Erkki Hellén: Nonequilibrium Dynamics in Fiber Networks, Aggregation, and Sand Ripples
ISBN 951-22-6161-8 (print)
ISBN 951-22-6162-6 (electronic)

OTAMEDIA OY
ESPOO 2002

Abstract

In nonequilibrium dynamical systems the rich macroscopic behavior arises from simple microscopic processes. While the dominant transport mechanism is often diffusion, there are important dynamics also beyond the diffusive scale. This thesis concentrates on these issues and the effects of spatial fluctuations in various nonequilibrium systems using computer simulations and theoretical arguments.

First, the combination of one-dimensional diffusion theory and random walk simulations is demonstrated to be a powerful tool for analyzing gas diffusion through paper-like structures. An efficient simulation method including the effects of fiber sorption is presented. When sorption is present, the characterization of dynamic diffusion processes is not possible using only the usually measured diffusion constant. The deviations between the theory and simulations suggest that the former is invalid for low porosities or thicknesses.

Next, the dynamical behavior in aggregation is considered within a one-dimensional model. This model, as in aggregation systems generally, obeys dynamic scaling described by a time-dependent, characteristic length. However, the first-passage quantities involve other scales. A novel mean-field theory is developed to extract the asymptotic time-dependence of unaggregated clusters, which is shown to relate to the small size tail of the cluster size distribution, a quantity of primary importance in aggregation. Then the effect of the presence of two scales on the dynamic scaling properties is discussed by considering the sites staying unvisited by clusters. When an external field like gravitation is applied, the aggregation dynamics is shown to be dominated by the process leading to the fastest growing characteristic length and the dynamic phase diagram is predicted.

Finally, coarsening of sand ripples is considered in one-dimensional mass transfer models motivated by sand ripple evolution. When mass is transferred preferably from large ripples to small ones, the ripple size distribution is calculated exactly and is given by a product measure. The approach towards the final state is discussed, leading to a universal decay which depends on the symmetry of the mass transfer. In the case of small clusters vanishing rapidly from the system, the noise in the dynamics is demonstrated to be irrelevant, but the mean-field theory developed fails to account for the numerically observed universality with respect to the initial ripple size distribution.

Preface

This thesis has been prepared in the Laboratory of Physics at the Helsinki University of Technology during the years 1998–2002.

I am deeply indebted to my supervisor Doc. Mikko Alava for his guidance during all the years in the Laboratory of Physics. In spite of his originality, he is excellent in those points which a supervisor should be good. I wish to thank Prof. Risto Nieminen for giving me the opportunity to carry out this work and for providing excellent working conditions. They are both also thanked for encouraging international interactions with other scientists and making them financially feasible. I am grateful to Doc. Kaarlo Niskanen and Dr. Jukka Ketoja from the KCL with whom I have had the pleasure to do physics connected to a fascinating material, i.e., paper. I would also like to thank Prof. Dr. Joachim Krug for the opportunity to visit him at the University of Essen, Germany, and for the fruitful collaboration. Working with the two other collaborators, Mr. Petja Salmi and Mr. Tapio Simula, has also been most enjoyable. I also wish to acknowledge many people, with whom I have had the privilege to discuss at conferences.

Furthermore, I would like to thank all the people of the Laboratory of Physics, which are too many to be listed here. I want, however, to mention and thank Dr. Eira Seppälä for useful conversations and for being the pioneer of the disordered materials group, and my roommates Dr. Andrés Ayuela and Mr. Jussi Enkovaara for a nice working atmosphere. I am also grateful to all of my friends and especially to my mother for her understanding of my enthusiasm on strange subjects (including physics) and for encouraging me on these.

The financial support by the National Technology Agency (TEKES), Academy of Finland's Center of Excellence program, Vilho, Yrjö, and Kalle Väisälä Foundation, Jenny and Antti Wihuri Foundation, Foundation of Technology, and DFG within SFB 237 is gratefully acknowledged.

Finally, my warmest thanks belong to my dear wife Heli, whose love and support are invaluable, and to my son Lauri, who has shown me that the greatest things of life have nothing to do with science.

Vantaa, August 2002

Erkki Hellén

Contents

List of Publications

This thesis consists of an overview and the following publications:

I. E. K. O. Hellén, J. A. Ketoja, K. J. Niskanen, and M. J. Alava, *"Diffusion through Fiber Networks"*, J. Pulp Pap. Sci. **28**, 55–62 (2002).

II. E. K. O. Hellén and M. J. Alava, *"Persistence in Cluster–Cluster Aggregation"*, Phys. Rev. E **66**, 026120-1–9 (2002).

III. E. K. O. Hellén, P. E. Salmi, and M. J. Alava, *"Cluster Survival and Polydispersity in Aggregation"*, Europhys. Lett. **59**, 186–192 (2002).

IV. E. K. O. Hellén, P. E. Salmi, and M. J. Alava, *"Cluster Persistence in One-Dimensional Diffusion–Limited Cluster–Cluster Aggregation"*, accepted for publication in Phys. Rev. E (11 pages).

V. E. K. O. Hellén, T. P. Simula, and M. J. Alava, *"Dynamic Scaling in One-Dimensional Cluster–Cluster Aggregation"*, Phys. Rev. E **62**, 4752–4756 (2000).

VI. E. K. O. Hellén and J. Krug, *"Coarsening of Sand Ripples in Mass Transfer Models"*, Phys. Rev. E **66**, 011304-1–9 (2002).

The author has had an active role in all the work reported in this thesis. He has been involved in planning the research program, in developing the calculations, and in interpreting the results. He has written the used computer programs himself except for the KCL-PAKKA program employed in generating the random fiber networks in Publication I and the random walk survival algorithm used in Publications III and IV. He has performed all the calculations and data analysis except for the comparison in Publication I and a part of the random walk analysis of Publications III and IV. The author has written the first drafts of Publications II–VI and partly that of Publication I, and contributed actively to the writing and publication processes.

1 Introduction

Nonequilibrium dynamical systems offer a challenge for statistical physicists. While the local dynamics is often formulated through a set of simple rules, the collective behavior is complicated and there is no general theory as for the equilibrium systems. Also, the range of applications is wide as the common features for various models are generally only stochasticity and transfer of particles. The fundamental transport mechanism is diffusion [1] and the richness in behavior is due to the interaction with the environment. This may be static as in the case of disordered media [2] or include dynamic changes as in growth and reaction-diffusion systems [3, 4].

One of the most important characteristics of the environment is its spatial dimensionality. For high enough dimensions mean-field theories, which are conceptually and mathematically simpler than those including spatial fluctuations, provide the correct description of the essential physics. However, in low dimensions spatial fluctuations can not be neglected and the behavior is different from that given by the mean-field analysis. The dimension below which a mean-field theory breaks down depends on the system considered. The fluctuations are the stronger the lower the dimension is and thus one-dimensional systems are optimal to study fluctuation effects [5].

In nonequilibrium systems the quantities of interest often obey dynamic scaling and systems are characterized through the related critical exponents. This is similar to the studies of critical phenomena, where universality plays a major role [6]. For a universal observable, it suffices to consider the simplest model obeying the right symmetries. The silent hope is that there would be similar underlying universality in nonequilibrium systems. Hence, a great deal of the studies on nonequilibrium dynamics, including those presented in this thesis, concentrate on simple models, which are hoped to capture the essential physics.

This thesis consists of studies on nonequilibrium dynamics and scaling in disordered and fluctuation-dominated systems in three and one dimensions, respectively. The background is introduced in this Section. Section 2 concentrates on diffusion through random fiber networks. In Sec. 3 three first-passage problems in diffusion-limited cluster-cluster aggregation are studied and Sec. 4 considers aggregation in the presence of an external field. Coarsening of sand ripples within simple mass transfer models is discussed in Sec. 5.

1.1 Diffusion and Random Walks

To start with, consider a diffusing particle in d-dimensional space. The probability density of finding the particle in position $\vec{r}$ at time t is given by the solution of the diffusion equation

$$\frac{\partial P(\vec{r};t)}{\partial t} = D\nabla^2 P(\vec{r};t), \tag{1}$$

where D is the diffusion coefficient. The diffusion process defined by Eq. (1) considers both space and time as continuous variables. However, many processes are conveniently described on a lattice and hence simulated using discrete random walks. On the other hand, theories are often simpler to formulate using the continuum description, i.e., diffusion. The random walk converges to diffusion in the limit $\Delta x \to 0$ and $\Delta t \to 0$ with $(\Delta x)^2/\Delta t$ fixed, where Δx is the lattice spacing and Δt is the time interval between consequent hops [1]. In practice this means that the long time, large scale properties obtained from random walk simulations should coincide with the continuum analysis.

The one-particle diffusion described by Eq. (1) and the corresponding random walk problem are readily solvable in a free space by various methods [1, 7]. The most important characteristics of diffusion are that the probability density is a Gaussian and the mean square displacement grows linearly, i.e. $\langle|\vec{r}(t) - \vec{r}(0)|^2\rangle \sim Dt$. The richness and complexity follows from the interaction with the environment. In most of the problems considered in this thesis a particle or a cluster of particles performs a simple random walk. When studying the diffusion of molecules through a paper-like structure (Section 2), both the disordered nature of the media and the molecule-fiber interaction make the issues nontrivial. In the part concentrating on cluster-cluster aggregation (Sections 3–4) the complications arise from interactions between clusters, which aggregate at contact. Finally, diffusion may be the most relevant transport mechanism only up to some crossover length or time scale after which the ballistic motion will dominate the dynamics (Section 4).

1.2 Diffusion in Paper

Paper is an excellent example of a disordered material, which can be produced in many different forms to fulfill the requirements of a vast variety

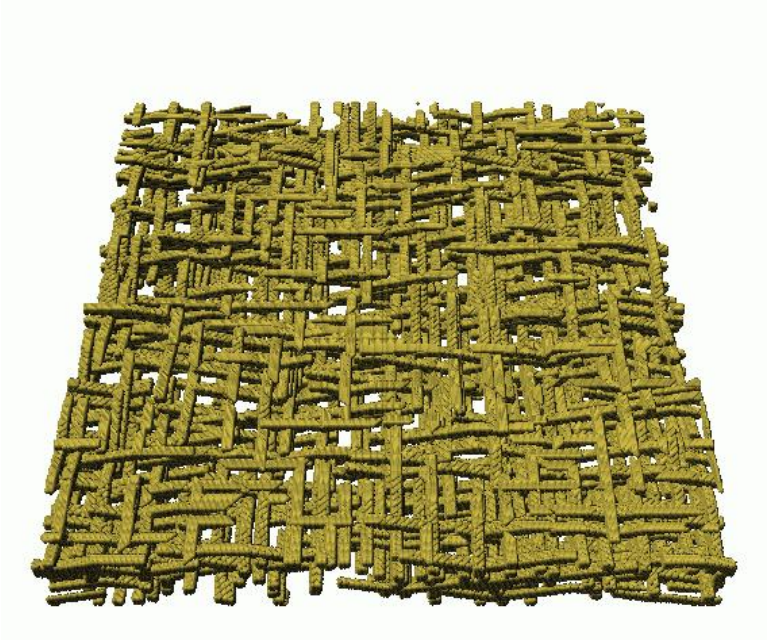

Figure 1: A sample of a thin random fiber network of porosity 0.83.

of everyday applications but whose physical properties are not completely understood [8, 9]. The problem with paper is that it usually consists of several types of fibers, fines and fillers, which form a disordered network. Even the characterization of such a structure has turned out be hard [8, 9]. Therefore, one needs simplified models which help to understand the basic characteristics. One such a model is the KCL-PAKKA [10], which produces random fiber networks that closely resemble real paper [11, 12]. Considering the transport properties, the permeability of KCL-PAKKA networks has been shown to behave similarly to that of paper and nonwoven fabrics over a large range of porosities [13].

Figure 1 shows an example of a random fiber network generated by the KCL-PAKKA program. The network consists of flexible fibers of rectangular cross-section. They are deposited one by one on an initially flat substrate. Each fiber is let to settle as low as possible without deforming the underlying sheet and obeying a flexibility constraint, which sets the maximum displacement of fibers per unit length. The porosity of networks can be varied by changing the fiber flexibility. The thickness of the resulting sheet is controlled by coverage, which measures the number of fibers per unit area. For a given fiber density the coverage is directly related to gram-

mage, which gives the mass per unit area. For more details of the sheet generation see Publication I.

In spite of the vast research on diffusion in disordered media [2, 4], most of the theories are not directly applicable to paper-like structures. A paper sheet consist of fibers, which have a high length-to-width ratio (typically about $50 - 100$ [8]), and therefore the resulting porous structure is highly anisotropic. Usually one is interested only in the transport through the sheet plane. As the typical thickness of paper is about 100 μm, it is not evident that the normal diffusion theory is applicable. Moreover, the fibers themselves have a porous structure and may also otherwise interact with the molecules diffusing in the web [14]. Article I focuses on these issues by studying diffusion through sheets generated by the KCL-PAKKA program.

1.3 Reaction-Diffusion Systems

When a diffusing particle reacts with its environment, which may be static or consist of other diffusing particles, and the reaction itself is fast enough, one speaks about reaction-diffusion systems. To be precise, this means processes, in which the timescale of reaction is much faster than the one by which particles come together. The basic reaction processes are capture, annihilation, coalescence, and aggregation, and the word diffusion stresses the fact that the overall kinetics is controlled by it.

In a capture process a particle gets trapped whenever it gets a contact with the environment. A classical example is the diffusion with static traps randomly distributed in space in which case a particle gets permanently captured when hitting a trap [2]. Also the problem of molecules diffusing through a paper sheet with fiber sorption included (studied in Section 2) falls into this category. The best known dynamic environment cases are perhaps predator-prey models, in which both species diffuse and predators kill preys [7]. The annihilating ($A + A \to \emptyset$) and coalescing ($A + A \to A$) random walkers are examples of reactions, in which particles either disappear at contact or merge on meeting [7]. Interestingly, in one dimension the dynamics of domain walls in the q-state Potts model, at zero temperature, can be represented as random walkers, which either annihilate or coalesce at contact with a q-dependent probability (see [15] and references therein). In the limit $q \to \infty$ the Potts model reduces to $A + A \to A$. The coalescence reaction itself is a simplification from the aggregation one, in which

the mass in the system is conserved and reactions are of type $A_i + A_j \to A_k$ with $k = i + j$, where the subscripts denote the masses of particles.

A part of this thesis concentrates on the aggregation process $A_i + A_j \to A_k$ where the diffusion constants depend on the masses of particles. The special case of mass independent diffusion corresponds to $A + A \to A$. When considering the probability of a cluster to remain unaggregated in Section 3.2, a three particle generalized diffusion-reaction system with annihilation at contact is used on a mean-field level. It should be noted that all the reactions described above are irreversible and occur when particles meet for the first time. Thus a useful perspective for understanding the kinetics of reaction-diffusion processes is provided by their first-passage properties. However, before discussing these let us introduce the diffusion-limited cluster-cluster aggregation model and discuss its scaling properties.

1.4 Diffusion–Limited Cluster-Cluster Aggregation

To understand the formation of complex, fractal structures in colloidal suspensions the diffusion-limited cluster-cluster aggregation (DLCA) model was developed in the 80's [16, 17]. It is defined by placing n particles to a volume V so that none of the particles overlaps. Particles and particle clusters move diffusively and the diffusion coefficient depends on the number of particles s belonging to a cluster. For clusters moving in a quiescent fluid it can be argued that the dependence is algebraic, $D(s) \sim s^{\gamma}$, and that the diffusion exponent γ should be inversely proportional to the fractal dimension of the clusters [18, 19, 20]. In the model the clusters are completely rigid and no particle rearrangement is allowed even at collisions. Whenever clusters (particles are clusters of size one) collide, they irreversibly aggregate together. In general, aggregates could also break into pieces, which may lead to a non-trivial steady state (see [21] and references therein). However, fragmentation is not considered in this thesis, and we concentrate on the one-dimensional DLCA for $D(s) \sim s^{\gamma}$ with γ being a free parameter.

For the three-dimensional DLCA the scaling properties of clusters and the dynamical scaling associated with the cluster size distribution are both well understood and consistent with experiments [22, 23]. The most famous theoretical approach to understand the dynamical behavior in aggregation is the Smoluchowski's rate equation theory [24]. Although it does not correctly describe the one-dimensional DLCA [25], we briefly outline it basic

features as it is generally applicable to various systems and also as the general structure of the solution is the same as that of the one-dimensional DLCA. When the concentration of particles is low enough such that only binary collisions need to be considered and one neglects spatial correlations between clusters, one arrives at

$$\frac{\mathrm{d}n_s(t)}{\mathrm{d}t} = \frac{1}{2}\sum_{i+j=s} K(i,j)n_i n_j - \sum_{i=1}^{\infty} K(i,s)n_i n_s, \tag{2}$$

where $n_s(t)$ is the number of clusters of size s at time t. All the interactions between clusters are hidden in the reaction kernel $K(i,j)$, which gives the rate at which clusters of size i and j aggregate.

As mean-field as the above approach may be, equations (2) form a hierarchy of differential equations, which can be analytically solved only for a few specific aggregation kernels [26, 27, 28]. Fortunately, when one is interested only in the large scale properties, there exists a powerful scaling theory for homogeneous kernels $K(ai, aj) = a^{\lambda}K(i,j)$ with $K(i,j) \sim i^{\mu}j^{\nu}$ ($i \ll j$; $\lambda = \mu + \nu$) [29, 30, 31]. For example, for mass-conserving systems the scaling form

$$n_s(t) = S(t)^{-2} f\left(\frac{s}{S(t)}\right) \tag{3}$$

has been verified through simulations and experiments [22, 23, 32]. The characteristic, time-dependent length scale is given by the average cluster size $S(t) \sim t^z$, where the dynamic exponent $z = 1/(1-\lambda)$ [33]. When $\lambda > 1$ the system gels, i.e., an infinite cluster is formed in a finite time. This thesis concentrates only on non-gelling systems, which requires $\gamma < 2$ for the one-dimensional DLCA.

The form of the scaling function $f(x)$ is sensitive to the value of μ and thus kernels are classified by it [29]. For class I kernels $\mu > 0$ and aggregation is dominated by the collisions of large clusters with large ones. In class III $\mu < 0$ and the aggregation is dominated by reactions between large and small clusters. Class II forms a marginal case, where the two processes are equally important. The small size tail $x \to 0^+$ of the scaling function behaves as $f(x) \sim x^{-\tau}$ in classes I and II and as $f(x) \sim \exp(-x^{-|\mu|})$ in class III. The polydispersity exponent τ is easily determined to be $\tau = 1 + \lambda$ in class I [29]. In contrast, calculating it for class II kernels would require the knowledge of the whole scaling function and provides still a challenge [34].

The DLCA kernels $K_D(i,j) \sim (i^{1/d_f} + j^{1/d_f})^{d-2}(i^\gamma + j^\gamma)$ $(d \geq 2)$ and $K_D(i,j) \sim (i^\gamma + j^\gamma)$ $(d = 1)$ belong to class II for $\gamma \geq 0$ and to class III $\gamma < 0$. Hence, in any dimension the mean-field theory predicts a transition between classes II and III at $\gamma = 0$ but according to (incorrectly interpreted) simulation results it has been argued to take place at a negative value of γ [35]. It has also been shown analytically that for the DLCA the upper critical dimension, above which the mean-field theory becomes exact, is infinite [31]. However, the deviations from it are, at reasonable time scales, negligible already in $d = 3$ [36].

The main problem in aggregation is to determine the exponents $(z, \tau, \ldots)$ and the scaling function $f(x)$. These play a similar role to the famous exponents of critical phenomena [6]. The most important issue is that both the exponents and the scaling function are universal. In other words, they are independent on the fine details of the model as well as on the initial conditions.

In addition to the exponents z and τ (or μ) the third exponent of interest is the decay exponent w, which describes the decrease of clusters of a fixed size, $n_s(t) \sim t^{-w}$. It is not independent of the others, and from Eq. (3) one easily obtains a scaling relation between the exponents [37, 29]

$$w = (2 - \tau)z, \tag{4}$$

when the scaling function decays algebraically at small argument values. However, the only readily calculable exponent for class II kernels is the dynamic exponent z. In Section 3.2 a different kind of a mean-field theory for the density of unaggregated clusters is developed, which for $\gamma \geq 0$ allows the determination of the exponent w for the one-dimensional DLCA.

1.5 First-Passage Problems and Persistence

In stochastic systems one is often interested in the distribution of events, when a variable reaches a specific value or state for the first time. These include chemical reactions, stock prices, diseases, and life time related issues to mention a few. When the distribution is normalized to unity, one speaks about the first-passage probability. Its integral provides the answer to the question "What is the probability, that something has *not* happened in a certain time interval?".

Due to the fundamental role of first-passage events they have been widely studied in reaction-diffusion systems, too. In one dimension several exact results exist. The most relevant for the present work are the following. For mass-independent diffusion, i.e. for $A_i + A_j \to A_k$, the cluster densities in DLCA decay asymptotically as $n_s(t) \sim t^{-3/2}$ [38]. The same result applies for the particle concentration in $A + A \to A$ [39, 7], for which system also the probability of a site to be unvisited by any particle has been calculated to decay asymptotically as t^{-1} [40]. Considering random walks, the survival probability of a single walker in the presence of an absorbing boundary decays as $t^{-1/2}$ [1, 7] and that of three annihilating random walkers as $t^{-3/2}$ at late times [41].

In spite of the number of exact results obtained, the systems are often far from trivial. Already the solution of the survival probability of three annihilating random walkers with unequal diffusion constants is rather involved [42] and the survival probability of a random walker in a deterministically expanding cage with absorbing boundaries has been solved only approximately [43]. The difficulties are not only analytical but also the approach to the asymptotic decay may be extremely slow. The best example is perhaps the survival of a diffusing particle among immobile or mobile traps. There exists analytical results [44, 45, 46] but verifying them by simulations has turned out to be hard [47, 48]. Lately it was argued that one would need to simulate probabilities less than 10^{-100} to see the true asymptotic behavior [49].

Many nonequilibrium systems obey dynamic scaling, i.e., a system will look the same if all the lengths are scaled by the time-dependent characteristic length. The advantage of the dynamic scaling is evident, for example, from the scaling form Eq. (3). It shows that the two-parameter function reduces to a one-parameter one with a dimensionless quantity as its argument. Hence, the time-dependence enters only through the characteristic length, which grows as a power of time and defines the dynamic exponent z. However, recently studies of first-passage properties under the name persistence have revealed that there may be another relevant length scales, whose behavior is not simply related to the one characterized by the dynamic exponent.

Let us give a concise introduction to persistence (for a short review see [50]). Consider a nonequilibrium field $\phi(x;t)$ fluctuating in space and time according to some specified dynamics. Persistence explores the fluctuations around the mean value and it is defined as the probability that at a fixed point in

space the quantity $\phi(x,t) - \langle\phi(x,t)\rangle$ has not changed sign up to time t. Often it measures the fraction of a system staying in its initial state, for example, in spin systems it may be the fraction of spins which have not flipped. When, as usually is the case [50], the persistence decays algebraically, $P(t) \sim t^{-\theta}$, the quantity of interest is the persistence exponent θ. As a great surprise, it turns out to be nontrivial even for a simple diffusion process as a result of the non-Markovian character of the problem [51, 52].

Since the introduction of persistence [53, 54] it has been studied a lot during the recent years, for example, in spin systems [15, 55, 56, 57, 58] and for growing interfaces [59, 60, 61, 62]. The interest stems from the fact that the persistence exponent is generally not related to the normal static or dynamic critical exponents. Especially, persistence is a quantity, which can not be tackled using correlation functions. For Markov processes persistence is relatively well understood [63, 64]. However, when the underlying process is non-Markovian, persistence gives information about the history of the system but the analytic analysis is difficult [51, 52, 65].

1.6 Beyond Diffusive Growth

In spite of its general importance, diffusion is not the only transport mechanism in aggregation systems. Consider, for example, the aggregation of particles in a suspension. In general, there are three forces acting on a particle (or a cluster consisting of particles): a gravitational force, an effective force due to the Brownian motion, and an effective force due to the interactions between particles [66]. If the clusters formed are small enough, roughly their radii being smaller than one micrometer, the system is dominated by diffusion and the results obtained from the DLCA model are consistent with the experiments [22, 23]. However, for larger aggregates gravitation becomes important and they undergo sedimentation. Although both the aggregation in suspensions and the sedimentation of non-Brownian particles have been studied extensively, the aggregation of fractals affected by the combined action of Brownian motion and gravity has been considered only recently [67, 68, 69, 70, 71, 72]. Most of these studies are related to the structure of aggregates. Section 4 and Article V concentrate on dynamic aspects by considering the dynamic scaling in cluster-cluster aggregation, in which clusters obey both diffusive and driven dynamics mimicking gravitation.

Another aggregation related coarsening process is considered in Section 5 and in Article VI. The main emphasis is on the role of the mass transfer in the evolution of sand ripples although the model considered has much in common with zero-range processes [73, 74, 75], urn models [76], and exclusion processes [74, 77, 78]. The basic difference, as compared to irreversible cluster-cluster aggregation, is that mass is migrated from a ripple to the neighboring one and ripples may also shrink in size. These type of nonequilibrium mass transfer models have various intriguing properties, for example, they may have many non-trivial steady states separated by phase transitions [79, 80]. On a mean-field level the general structure of migration-driven growth was recently shown to besimilar to that of conventional aggregation [81]. However, the system studied in this thesis is one-dimensional and fluctuations play a crucial role.

2 Diffusion through a Paper Sheet

In this Section diffusion through a disordered fiber network is studied. The aim is to understand how gas penetrates through a paper sheet and, especially, how the sorption properties of fibers affect the transport. Understanding diffusive transport is important in many papermaking operations and end uses of paper and board. Examples range from moisture and heat conduction in drying, coating, calendaring and printing to the migration of organic compounds in food packaging materials. The sorption by fibers is in turn significant because, in the cases of practical interest, the diffusion field often has not yet saturated to a steady state. This is the case, for example, in processes in which water is applied or removed from a running web in a printing press. On the other hand, measuring diffusion experimentally is tedious [82, 14].

Here a combined method using both analytical and numerical analysis for extracting the entire first-passage time distribution (in the following called flux) of molecules through a paper sheet is introduced. The flux is calculated from an extended one-dimensional diffusion equation theory, which includes the effect of fiber sorption. The calculated flux is then fitted to the one obtained from simulations, in which random walkers wander through a computer generated random fiber network. The fitting parameters are the diffusion constant D and the ratio of sorption and desorption constants of fibers. The method is both fast and cost-efficient in evaluating the effect of constituents, i.e. furnish composition, and sheet structure on diffusion. The results from computer simulations and diffusion theory are compared to experimentally measured diffusion constants of paper sheets and board with a good agreement.

2.1 An Efficient Simulation Algorithm

The networks are generated using the KCL-PAKKA program shortly described in Section 1.2. A typical network is presented in Fig. 1. In simulations the space enclosing the network is divided into a simple cubic lattice with a lattice constant of 1 μm. Initially all the diffusing molecules are, say, on the lower side of the sheet. The concentration of molecules is low and they are considered as independent random walkers, which move only in the empty sites containing no fibers. The main simplification is that the

interaction between a molecule and a fiber only causes a time delay in its motion, i.e., when a walker hits a fiber surface, it has to wait some time before taking the next step. This mimics a situation, in which a molecule gets adsorbed on the fiber surface and later desorbs from it. However, the method probably fits also to cases when molecules diffuse along fiber walls or inside the fiber lumen. This is since the fibers are aligned mainly horizontally and desorption occurs on the average at the same height as sorption.

The simulation method introduced in Article I for the specific geometry in question has two main ingredients, which increase its efficiency as compared to simple random walk methods usually described in the literature [83, 84]. First, a random walker invading to the web has a high probability to come out from the web to the same side from which it went in. After this it may return to the web quickly or wander a long time below the network before entering it again. These excursions affect the time distribution of penetrating walkers but they are irrelevant when considering the effect of the network on diffusion, which is what we are interested in. Therefore, each random walker that tries to walk in the space below the web is returned to its lower surface. This has to be done so that it does not affect the flux at the top boundary of the sheet, which requires the calculation of both the first-return time distribution and the conditional spatial distribution of returns after a given time. The analytical calculations detailed in Article I are elementary but lead to rather cumbersome results. Nevertheless, the algorithm utilizing them is about 100 times faster than the one in which particles are allowed to walk also below the web. Similar ideas have been used in the studies of the conductivity, dielectric constant and diffusion in digitized composite media [85] and in the generation of large diffusion-limited aggregation clusters [86, 87].

The second technique increasing computational efficiency is similar to that used when studying diffusion on percolation clusters [88]. Instead of using a "blind" walker, which first selects a random direction and then decides if it is possible to hop to that direction, one uses a "myopic" walker, which at every step selects a direction from the allowed ones. The amount of time the move requires depends on the number of allowed directions. Here the method is generalized to take into account the sorption interaction between the random walkers and fibers: a random walker entering a site takes the next hop after an average time, which depends on the local configuration $\mathcal{C}$ around that site. When the web consist of n fiber types with each having a different set of sorption parameters, there are $(n+1)^6$ different surrounding

configurations for a molecule on a three-dimensional cubic lattice. When the sorption to desorption ratio of fiber type i is denoted by $\hat{\nu}_i$, the average residence time is calculated to be

$$\bar{t}(\mathcal{C}) = \frac{6 + \sum_{i=1}^{n} \hat{\nu}_i k_i(\mathcal{C})}{6 - \sum_{i=1}^{n} k_i(\mathcal{C})}, \tag{5}$$

where $k_i(\mathcal{C})$ is the number of fibers of type i in the nearest neighbor sites of the molecule in configuration $\mathcal{C}$.

As an example, a sheet of porosity 0.57, grammage 60 g/m^2, and cross-sectional area of 0.09 cm^2 corresponds to 1.3×10^9 diffusion cells of size 1 μm and requires only some 60 Mb of RAM memory. Using the algorithm described above, it takes about 100 minutes of CPU-time on a personal workstation with 500 MHz Alpha processor to make 10000 random walkers to penetrate through this web.

2.2 One-Dimensional Diffusion Theory Including Fiber Sorption

Consider a paper sheet of porosity ϕ as a one-dimensional effective medium and denote the concentration of molecules in the pore and fiber spaces by C_p and C_f, respectively. Then the diffusion-sorption process inside the network can be represented by the coupled partial differential equations

$$\frac{\partial C_p(z,t)}{\partial t} = D\frac{\partial^2 C_p(z,t)}{\partial z^2} - \frac{\partial C_f(z,t)}{\partial t} \tag{6}$$

$$\frac{\partial C_f(z,t)}{\partial t} = \lambda C_p(z,t) - \mu C_f(z,t), \tag{7}$$

where z gives the distance from the bottom surface of the sheet, D is the diffusion constant, and λ and μ denote the sorption and desorption rates, respectively. Outside the network the concentration satisfies the standard diffusion equation

$$\frac{\partial C(z,t)}{\partial t} = D_g \frac{\partial^2 C(z,t)}{\partial z^2}, \tag{8}$$

where D_g is the molecular diffusion constant in the free space (e.g. air). The system of equations is linear and can be solved using the Laplace transformation. When sorption is present, the solution will be a rather cumbersome and not very illuminating expression, which, however, is easily handled with

Mathematica, for example. In the absence of sorption ($\lambda = \mu = 0$) the solution is relatively simple and the flux at the top sheet boundary $z = a$ takes the form

$$H(t) = -D \left.\frac{\partial C_p}{\partial z}\right|_{z=a} = \frac{2\phi C_0 D}{a(1+\phi\sqrt{D/D_g})\sqrt{\pi t'}} \sum_{n=0}^{\infty} (-1)^n \alpha^n e^{-\frac{(2n+1)^2}{4t'}}, \quad (9)$$

where $t' = Dt/a$ is dimensionless time, C_0 is the initial concentration below the sheet, and $\alpha = (\phi - \sqrt{D_g/D})/(\phi + \sqrt{D_g/D})$.

The two essential parameters characterizing the sheet in the theory are thickness and porosity. As real sheet surfaces are rough there is no unique way of determining these parameters. We tried several definitions, and the best match between the theory and simulations was obtained using the apparent thickness a and porosity ϕ. The first one is defined so that 80 % of local thickness values are below a. The corresponding apparent porosity $\phi = 1 - \rho/\rho_f$, where ρ_f is fiber density and ρ equals grammage divided by a. These quantities also have the pleasant aspect of being experimentally easy to measure.

2.3 Comparison between Simulations, Theory, and Experiments

In simulations the sheet consists of one fiber type with density 1400 kg/m^3, length 2 mm, thickness 4.3 μm, and width 40 μm. This corresponds roughly to a paper made from relatively stiff Nordic softwood fibers. The parameter controlling fiber flexibility, the ratio of pressure (representing all the compressive effects of wet pressing) over fiber shear modulus, is in the range $0.075 - 0.830$. This leads to sheet density variations of $400 - 1000$ kg/m^3 and porosities $0.3 - 0.7$.

In figure 2 the rescaled flux $H' = Ha/(C_0 D)$ is compared to the one obtained from simulations when there is no sorption. The only fitting parameter is the diffusion constant D, which is determined by the saturated flux. For thick sheets with large porosities the flux calculated from the theory agrees well with the one obtained from simulations for all times. On the other hand, for thin sheets or small porosities the flux given by Eq. (9) rises more slowly than it should. The threshold grammage above which the theory is valid increases as porosity decreases. The actual dependence was not analysed

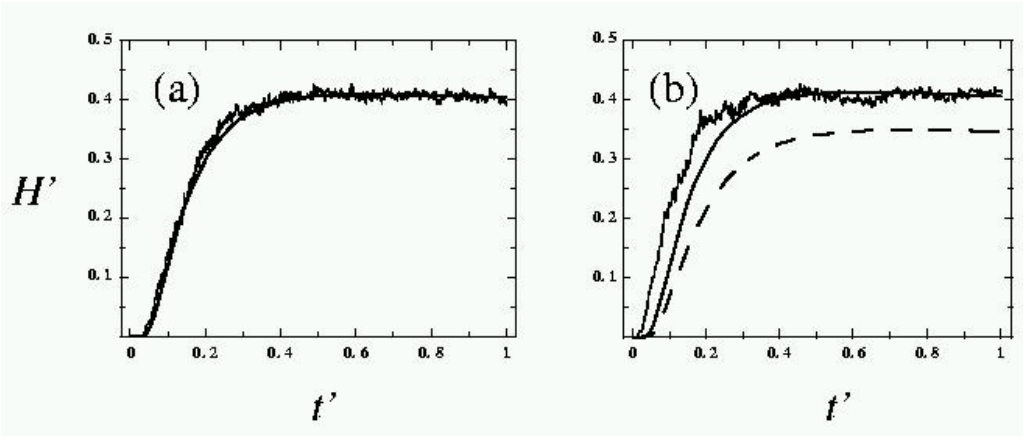

Figure 2: Comparison of the simulated flux (rough lines) to Eq. (9) (solid line) for two sheets of approximately of the same porosity. The flux H is rescaled to $H' = Ha/(C_0 D)$, which is presented as a function of the dimensionless time $t' = Dt/a$. In (a) the sheet is thick ($a = 369$ μm; $\phi = 0.485$) and in (b) thin ($a = 47$ μm; $\phi = 0.463$). The fitted diffusion constant is (a) $D = 0.0545 D_g$ and (b) $D = 0.0659 D_g$. For comparison the dashed curve shows the flux calculated from the one-dimensional theory with the same diffusion constant as in (a).

in detail but the threshold grammage is certainly larger than the one at which the network crosses over from a vacancy-controlled two-dimensional structure to a pore-controlled three-dimensional one [11]. Above the latter threshold the number of pores increases linearly with coverage.

There are several possible explanations for a discrepancy between the simulations and analytical results. First, the simulated network is built on a flat surface and hence the asymptotic bulk behavior is not reached for low coverages. Therefore, there are porosity gradients near the bottom surface not taken into account in the theory. In other, more simple systems such as composite media, the spatial variation in the transport properties of the material is known to modify the first-passage behavior in a non-trivial and complicated manner [7]. Second, for low grammages the probability to have direct holes through the sheet is not negligible, which can cause the initial flux to rise faster than predicted by the theory. Third, for low porosities statistical fluctuations in sheet structure become important and alter the transport behavior. As known from percolation theory, diffusion is anomalous up to a porosity dependent crossover length scale for systems near the

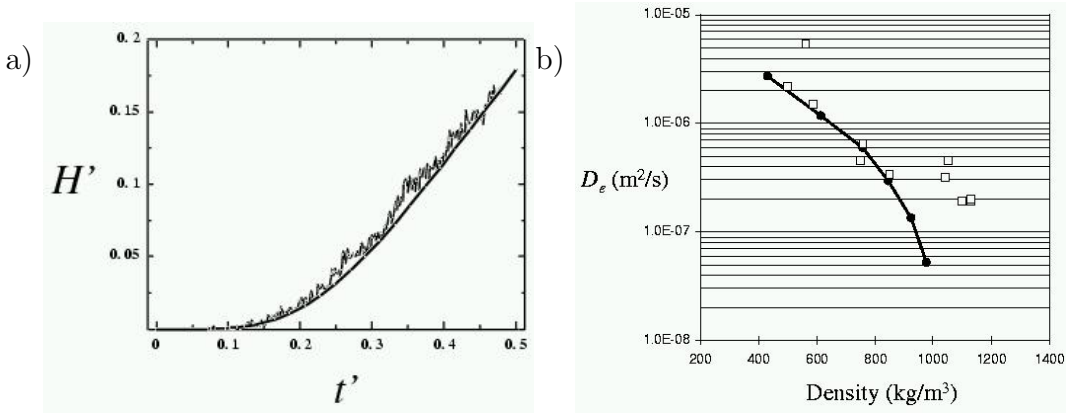

Figure 3: a) Comparison of the simulated flux (rough line) to the one-dimensional theory (solid line) with relatively large fiber sorption. The parameters are $\hat{\nu} = 50$, $a = 582$ μm, $\phi = 0.691$, $D = 0.163 D_g$, and $\lambda = 0.0002$. b) Behavior of the effective diffusion constant as a function of apparent sheet density. Solid circles are obtained by fitting the theoretical flux to the simulated one and open rectangles represent the experimental values [89].

percolation threshold [90]. Finally, near the bottom surface there may also be shallow pores between almost parallel fibers which act like traps for the molecules.

As a consequence of the above reasons, the effect of fiber sorption is analyzed using thick sheets of large porosity. Naturally sorption changes only the early time part of the flux and leaves the large time tail characterized by the diffusion constant unaffected. The two parameters characterizing the sorption in the theory are λ and μ. The ratio of these is, within the numerical accuracy, related to the corresponding parameter $\hat{\nu}$ used in the simulations as

$$\frac{\lambda}{\mu} = \hat{\nu} S, \tag{10}$$

where S is the free specific surface area of fibers (free surface area divided by the pore volume). Fixing the value of λ a good match between the theory and simulations is obtained varying only S for all porosities and sheet thicknesses. Figure 3a shows an example of the fit for $\hat{\nu} = 50$, $\phi = 0.691$, and $a = 582$ μm. Note that the sorption and desorption terms in Eq. (7) are essential and getting a good match between simulations and theory by

using the result given by Eq. (9), i.e. $\lambda = \mu = 0$, is impossible.

Figure 3b compares the simulated effective diffusion constant $D_e = \phi D$ to experimentally measured water vapor diffusion of various uncoated pulp and paper samples. The comparison is between the orders of magnitudes as no attempt to reproduce the actual sheet structure is made in simulations. Nevertheless, the agreement is good, especially for low density sheets. The deviation at high densities may be due to the fillers in real sheets, which increase the density in a different way than fibers.

Recent experiments have further shown that the diffusion flux is sensitive to molecules that diffuse in the sheet [91, 82]. For example, the experimentally measured diffusion constant for butanol is, within the measurement error, the same than that given by the theory and simulations but ethanol diffuses about four times faster than predicted. Note, however, that we have here concentrated only on diffusion through the pore phase. It is known that at high relative humidities the diffusion along fiber walls becomes the dominant transport mechanism [14, 92]. A possible explanation for the difference might thus be the diffusion of molecules along fiber surfaces, the rate of which is molecule dependent.

In conclusion, the one-dimensional diffusion theory is not valid for thin sheets at low porosities. The deviations from the theoretical predictions are significant as the interesting cases often involve dynamic processes. Although no detailed estimation of the threshold was done, it seems that ordinary 60 g/m^2 handsheets are always too thin for the theory to apply. However, the results for thick and porous sheets indicate that gas diffusion through paper and board sheets can be efficiently simulated using model fiber networks, also in cases including fiber sorption.

3 First-Passage Problems in Aggregation

As discussed in Section 1.4, aggregation models often lead to scale-invariance: the average cluster size increases as a power-law $S(t) \sim t^z$, which defines the dynamic exponent z. This kind of behavior is met in various contexts ranging from chemical engineering to material sciences to atmosphere research to even astrophysics [22, 32, 93]. The power of dynamic scaling is based on the assumption that there is a single, characteristic length scale given by $S(t)$. However, studies of nonequilibrium dynamics in various systems have shown that quantities related to first-passage events may not be directly related to that [50]. It is thus natural to consider dynamics in aggregation beyond the length and time scales governed through z.

In an aggregation system one can define many first-passage problems, which allows one to probe the dynamics from different viewpoints. Here we concentrate on three first-passage probabilities in the one-dimensional diffusion–limited cluster–clusters aggregation when the diffusion coefficient of a cluster depends on its size as $D(s) \sim s^\gamma$. Figure 4 visualizes the dynamics and shows some of the first-passage quantities studied.

Simulations are done on a lattice and two first-passages problems related to lattice sites are discussed in Section 3.1. The probability of an occupied site to remain ocuupied is demonstrated to be nonuniversal and is commented upon only briefly. The empty site persistence, which gives the probability that a site has never been visited by a cluster, is shown to be universal. The corresponding persistence exponent turns out to be twice the dynamic exponent. Thus the associated length scale becomes clearly visible in the scaling of the interval size distribution, which is not always the case [40].

Section 3.2 generalizes persistence to clusters, i.e., the probability of a cluster to remain unaggregated is studied. In the mean-field limit the problem is reduced to the survival of three random walkers with time-dependent noise correlations. In spite of the fluctuation dominated dynamics, the random walk approach captures the essential features for $\gamma \geq 0$ and gives qualitative understanding of cluster persistence for $\gamma < 0$. The solution of the cluster persistence relates to the behavior of the small size tail of the cluster size distribution, which is of primary interest in aggregation systems and can not be tackled using the traditional mean-field theory introduced in Sec. 1.4. The results are reported in detail in Publications II, III, and IV.

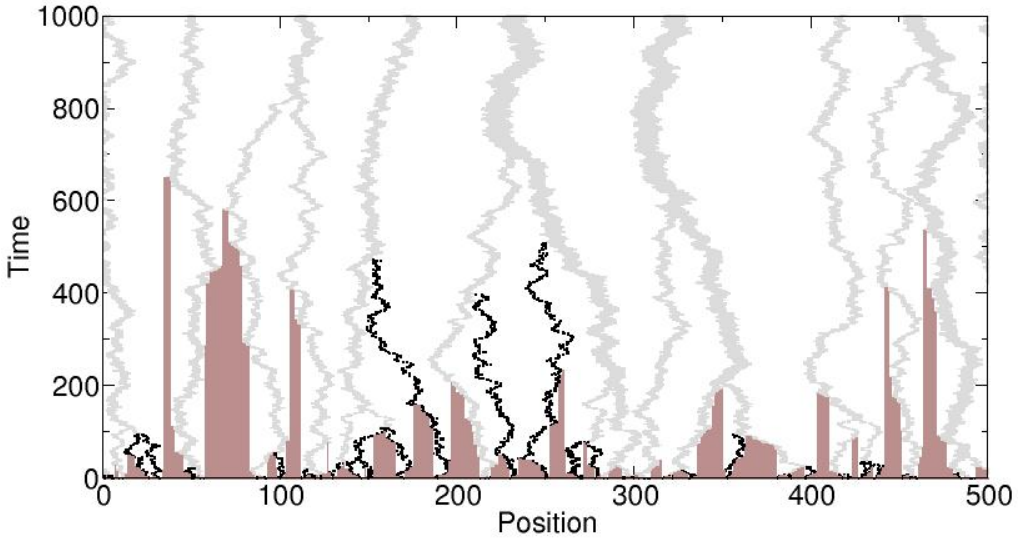

Figure 4: A space-time plot of the dynamics in one-dimensional diffusion-limited cluster-cluster aggregation when the diffusion coefficient of a cluster is independent of its size. The figure illustrates two first-passage quantities, the unaggregated clusters (denoted by black) and the regions never visited by any of the clusters (brown areas). Aggregated clusters are denoted by light gray.

3.1 Persistence at a Fixed Lattice Site

The most commonly used definition for persistence considers the fraction of a system staying in its initial state. For the DLCA the natural quantities thus are the empty and filled site persistences $P_E(t)$ and $P_F(t)$, which give the probabilities that an originally empty site has never been occupied by a cluster and that a site originally covered by a cluster has been covered by it all the time, respectively.

Consider first the empty site persistence. Since clusters move independently and can not aggregate, in one dimension, without making all the sites between their initial positions non-persistent, each persistent empty region is shortened by two independent processes (clusters). For size-independent aggregation the problem reduces to the exactly solvable reaction–diffusion system $A + A \to A$ and $P_E(t) = \langle k_0^2 \rangle / (2\pi t)$, where $\langle k_0^2 \rangle$ is the averaged squared length of the initial empty region distribution [40]. Hence, the ini-

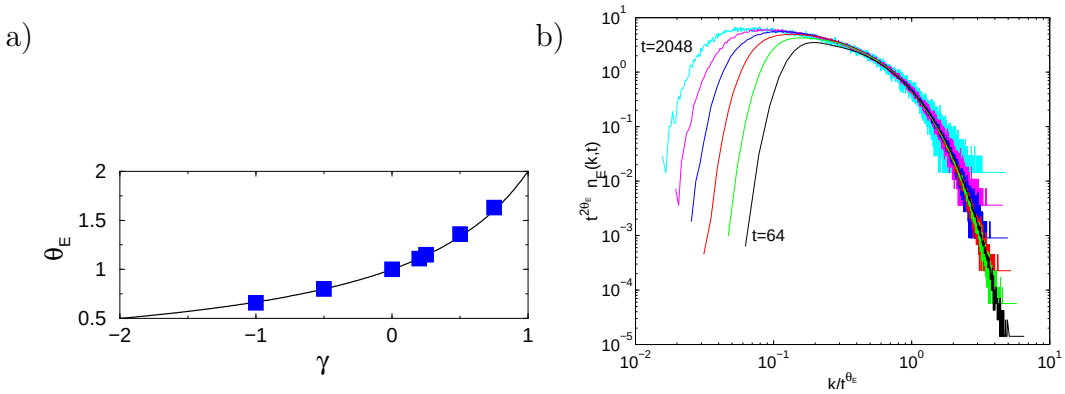

Figure 5: a) Comparison of the numerically obtained empty site persistence exponent θ_E (■) to the mean-field result $\theta_E = 2z = 2/(2-\gamma)$ (solid line). b) Scaling plot for the interval size distribution between two consecutive persistent empty sites at $t = 2^6, \ldots, 2^{11}$ for $\gamma = 0$. The poor scaling at small k/t^{θ_E} is due to the competition of the length scales t^{θ_E} and t^z.

tial distribution affects only the amplitude of the universal decay $\sim t^{-1}$. When $\gamma \neq 0$ and clusters are considered to behave in an average way, i.e., each cluster is taken to diffuse with a time-dependent diffusion coefficient $D(t) = D_0 t^{\gamma z} \sim S(t)$, the result will remain the same except that the time scale t gets modified to $T = D_0 t^{\gamma z+1}/(\gamma z + 1)$. The resulting mean-field result $P_E(t) \sim t^{-\theta_E}$ with $\theta_E(\gamma) = 2z = 2/(2-\gamma)$ agrees well with the simulation results as shown in figure 5a. Simulations also confirm the independence of the persistence exponent of the initial spatial distribution and concentration.

Although the persistence exponent is universal, the size distribution of persistent regions, $p_E(r;t)$, depends on the initial condition. However, the spatial and time dependencies are decoupled, i.e., $p_E(r;t) = p_1(r)p_2(t)$, which explains the universality of the persistence exponent. The decoupling also implies that the average region size is constant at late times.

More interesting than the nonuniversal region size distribution is the interval size distribution measuring the distances between persistent regions. It scales universally as

$$n_E(k;t) = K_E(t)^{-2} e^{-k/K_E(t)}, \tag{11}$$

where $K_E(t) \sim t^{\theta_E}$ denotes the average interval size. The simple exponential

decay is due to the uncorrelated nature of the processes making the intervals shorter: the correlations grow as the diffusive length scale t^z but at late times the persistent regions will be well separated since the persistence scale $t^{\theta_E} \gg t^z$. However, at any finite time the presence of the two length scales affects the scaling of Eq. (11). For example, in the diffusion–reaction model $A+A \to \emptyset$ the empty site persistence was first found to be nonuniversal [94, 95, 96]. Afterwards the same authors argued for universality and claimed the poor separation of the scales to be the origin of the confusion [97, 98]. Such an effect was also suggested to be the reason for the poor scaling of the interval size distribution between the persistent regions in the one-dimensional q-state Potts model [40]. However, in neither of these systems is the length scale separation evident. In the DLCA the effect of the two lengths is clearly visible as Fig. 5b demonstrates. The large length tail of the interval size distributions scales nicely but the short interval part does not collapse on one curve. The scaling works for $k/t^{\theta_E} \gg t^{-z}$ and hence the diffusive scale becomes irrelevant at the long time limit.

In contrast to the empty site persistence the decay of the filled site persistence depends on concentration. At high concentrations this is understandable as the average distance between clusters is smaller than the average cluster size and a cluster generally aggregates with its neighbor before the sites under it lose their persistence. Hence, a large cluster contains many persistent regions inside it but only the regions near the edges of a cluster are affected by its motion. On the other hand, at low concentrations a persistent region usually gets destroyed before the cluster containing it aggregates.

Within the approximation that the collisions between clusters do not matter the persistence probability is given by

$$p_F(t) = \int_0^\infty \mathrm{d}s \; p_F(t|s) n_s(0), \tag{12}$$

where $p_F(t|s) \approx 8Dts^{-2} \exp\{-\pi^2 Dt/(2s^2)\}$ is the leading order term of the probability of finding persistent sites inside a cluster of size s. Hence, the persistence probability depends on the initial cluster size distribution and decays generally stretched exponentially $p_F(t) \sim t^{\beta_1} \exp(-At^{\beta_2})$ with concentration dependent exponents β_i. Simulations show that this is true only up to a concentration dependent crossover time scale $\sim 1/(D\phi)$ after which the collisions between clusters become significant. Asymptotically the persistence probability decays as a power law $P_F(t) \sim t^{-\theta_F}$, where the

exponent θ_F depends on concentration. Similar nonuniversal persistence has been observed also in anisotropic coarsening of polycrystalline grains [99] and in vortex dynamics of the two-dimensional XY-model [100].

3.2 Cluster Persistence

The empty and filled site persistences characterize first-passage probabilities at a fixed lattice site. Cluster persistence differs from these as it considers a first-passage problem related to clusters: it is defined as the probability $P_C(t)$ that a cluster has not aggregated. As such, it is related to the essential issue of the shape of the cluster size distribution.

3.2.1 Mean-Field Random Walk Approach

To understand the decay of cluster persistence we start by considering a mean-field method resembling that used in the analysis of the empty site persistence. Similarly to the persistent sites also the persistent clusters are well separated at late times, i.e., there will be many nonpersistent clusters between two persistent ones. Hence, each persistent cluster loses its persistence independently of the others and one can concentrate on the behavior of one persistent cluster surrounded by two nonpersistent ones. The finite extent of clusters is irrelevant and they can be considered as point particles with positions $x_1(t) \leq x_2(t) \leq x_3(t)$. Making the mean-field approximation that the neighboring clusters grow as an average cluster does ($S(t) \sim t^z$) leads to time-dependent diffusion coefficients for the neighboring particles: $\mathcal{D}_1(t) = \mathcal{D}_3(t) = D_1 t^{\gamma z}$. These particles will follow a simple diffusion with a constant diffusion coefficient D_1 in the time scale $T(t) = t^{\gamma z+1}/(\gamma z + 1)$.

The behavior of the three particle system is described by the Fokker-Planck equation

$$\frac{\partial \rho}{\partial t} = (D_2 + D_1 t^{\gamma z}) \left(\frac{\partial^2 \rho}{\partial x_{12}^2} + \frac{\partial^2 \rho}{\partial x_{23}^2} \right) - 2D_2 \frac{\partial^2 \rho}{\partial x_{12} \partial x_{23}}. \tag{13}$$

where $\rho(x_{12}, x_{23}; t)$ is the probability density to have distances $x_{12}(t) = x_2 - x_1$ and $x_{23}(t) = x_3 - x_2$ at time t and D_2 is the diffusion constant of the particle corresponding to the persistent cluster. As a cluster becomes nonpersistent when it collides with either of its neighbors, Eq. (13) should be solved with absorbing boundary conditions along the axis, i.e., $\rho(x_{12}, 0; t) =$

$\rho(0, x_{23}; t) = 0$ for all times t. The initial distance distribution between clusters gives the initial condition, which for the simplest case of equidistant clusters reads as $\rho(x_{12}, x_{23}; 0) = \delta(x_{12} - x_{12}(0))\delta(x_{23} - x_{23}(0))$. The survival probability

$$P_{\mathrm{surv}}(t) = \int_0^\infty dx_{12} \int_0^\infty dx_{23} \rho(x_{12}, x_{23}; t) \tag{14}$$

provides the mean-field approximation to the persistence probability $P_C(t)$. When these decay algebraically, the associated exponents θ_{RW} and θ_C are called survival and cluster persistent exponents, respectively. In other words, on the mean-field level the problem of cluster persistence reduces to the survival of three annihilating random walkers with time dependent noise correlations.

3.2.2 Mean-Field is Adequate ($\gamma \geq 0$)

For size independent diffusion ($\gamma = 0$) both the one-dimensional DLCA and the corresponding three particle random walk problem are exactly solvable [38, 41, 101]. The survival and persistence probabilities coincide and $P_{\mathrm{surv}}(t) = P_C(t) \sim t^{-3/2}$, which can be obtained also from Eqs. (13) and (14). Unfortunately, for $\gamma \neq 0$ the equation (13) with absorbing boundary conditions is not tractable by standard techniques [102]. For $\gamma > 0$, it can be solved in the limit $t \to \infty$ and $P_{\mathrm{surv}}(t) \sim t^{-\theta_{RW}}$, where $\theta_{RW}(\gamma) = 2z = 2/(2 - \gamma)$. Simulations confirm the result for the survival and show that the persistence decays with the same exponent (see Fig. 6) although the crossover effects make the analysis intractable near $\gamma = 0$. As demonstrated in Publication IV, for $\gamma \neq 0$ the corrections to the leading order asymptotic behavior go in powers of the ratio of the diffusion coefficients $D_2/(D_1 t^{\gamma z})$. As a consequence, the corrections become negligible for times much larger than the crossover time $t_{\mathrm{cr}} \sim r^{(2-\gamma)/|\gamma|}$, where $r \approx 30$ is a constant. Hence, t_{cr} diverges as $\gamma \to 0$. This differs drastically from the $\gamma = 0$ behavior, in which case $t_{\mathrm{cr}} = 3l_0/(16D)$, where l_0 indicates the initial distance between particles and D is the diffusion constant [101, 38].

The persistence exponent is discontinuous and non-monotonic as $3/2 = \theta_C(0) > \theta_C(0^+) = 1$. Thus, we arrive at the non-intuitive result that making some of the clusters to diffuse faster helps the others to stay longer intact. The reason for the peculiar behavior is that the persistent clusters become slower than the average ones and eventually adopt the optimal survival strategy [103] by becoming stationary. This interpretation is further

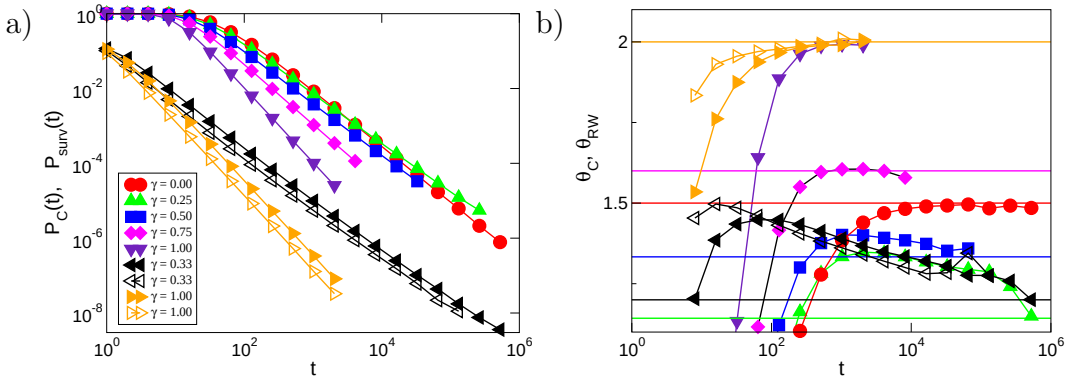

Figure 6: a) Comparison between the survival (filled symbols) and cluster persistence (open symbols) probabilities. The lower (upper) curves correspond to the initial distance between particles being 2 (10). b) The corresponding local exponents. The horizontal lines show the analytic predictions given by $\theta_C = 2/(2-\gamma)$.

supported by the fact that the cluster and empty site persistences decay with the same exponent for $\gamma > 0$. Note that asymptotically the persistence probability decays similarly to the joint survival probability of two independent random walkers diffusing with diffusion coefficients $\mathcal{D}(t) \sim t^{\gamma z}$ with a fixed absorbing boundary in between. This implies that the fluctuations in the motion of the slow, persistent clusters become irrelevant for $\gamma > 0$ in the limit $t \to \infty$ although the aggregation itself is dominated by spatial fluctuations [25].

3.2.3 Fluctuation Dominated Persistence ($\gamma < 0$)

The simple asymptotic analysis of Eq. (13), which provides the correct result for $\gamma > 0$, does not adequately describe the persistence for $\gamma < 0$. It leads to an exponential decay but simulations show that both the survival and persistence probabilities decay stretched exponentially, $P_{\rm surv}(t) \sim \exp(-C_{\rm RW} t^{\beta_{\rm RW}})$ and $P_C(t) \sim \exp(-C_{\rm C} t^{\beta_{\rm C}})$, respectively. The stretching exponents are independent of initial conditions, and for the persistence numerics suggest an expression $\beta_C = 2(1-2z)/3$ whereas for the survival $\beta_{\rm RW} = (1-2z)/2$ with $z = 1/(2-\gamma)$ (see Fig. 7a).

Next we present a Lifshitz tail argument [7], which heuristically explains the functional dependence of the survival stretching exponent $\beta_{\rm RW}$ on the

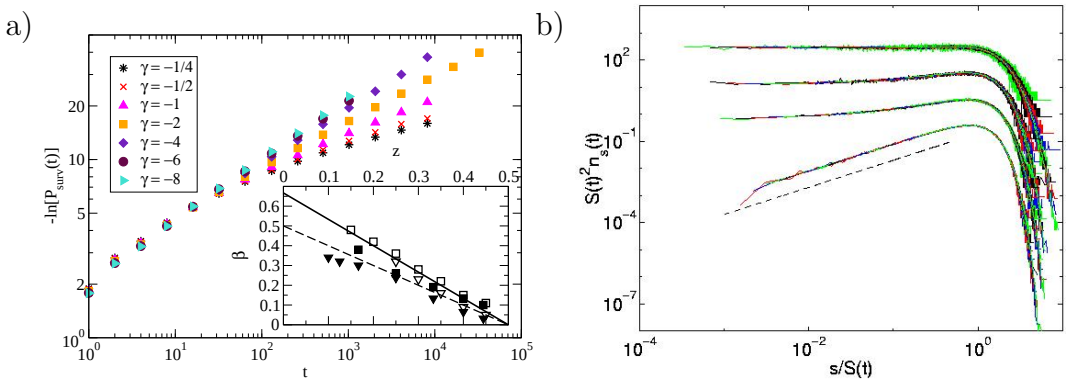

Figure 7: a) The survival probabilities for $\gamma < 0$. A straight line corresponds to a stretched exponential decay with the slope giving the stretching exponent $\beta_{\rm RW}$. The inset shows bounds for the survival (filled symbols) and persistence (open symbols) stretching exponents as a function of the dynamic exponent. The dashed and solid lines are given by $\frac{1}{2}(1-2z)$ and $\frac{2}{3}(1-2z)$, respectively. b) The scaling plot for the cluster size distribution for $\gamma = 0.00, 0.40, 0.57$, and 1.00 (from bottom to top) showing that $\tau = 0$ for $\gamma > 0$. The dashed line has a slope 1 and the distributions (except the $\gamma = 0$ one) have been shifted in the vertical direction for clarity.

dynamic exponent z and gives hints, why the mean-field theory fails for $\gamma < 0$. The argument assumes that a relatively small number of extreme configurations provides the main contribution to the asymptotic survival probability. In the three particle random walk problem these configurations are those, in which the particles surrounding the surviving one have diffused far apart from each other. Hence, within the Lifshitz approach, the survival probability can be written as

$$P_{\rm surv}(t) \approx \int_0^\infty {\rm d}l \; P(l;t) Q(t|l), \tag{15}$$

where $P(l;t)$ is the probability distribution of the interval lengths $l = x_3 - x_1$ around a surviving particle at time t and $Q(t|l) \sim l^{-1} \exp(-\pi^2 D t/l^2)$ is the dominant large time term of the survival probability of a particle in an interval of length l [7, 1].

To proceed, we need to know the large l behavior of $P(l)$. According to the simulations it scales as

$$P(l;t) = t^{-z} G\left(\frac{l - 2bt^\alpha}{t^z}\right) \tag{16}$$

similarly to the reaction front in the initially separated reaction-diffusion system $A + B \to C$ [104, 105]. Here b is a constant, α is a non-trivial exponent describing the growth of the mean interval length, and the large y tail of the scaling function $G(y)$ is Gaussian. Consequently, Eq. (15) gives

$$P_{\rm surv}(t) \sim t^{(6z-1)/4} e^{-Ct^{(1-2z)/2}}, \tag{17}$$

in agreement with the numerical result $\beta_{\rm RW} = (1-2z)/2$.

A few points on this result are worth noticing. First, the argument of the exponential decay is simply the ratio of the two length scales in the problem: the one related to the random walkers with time-dependent diffusion coefficients, $L_1 \sim t^z$, and the other to the surviving particle $L_2 \sim t^{1/2}$. Second, the same result for the stretching exponent can be obtained by considering the survival of a random walker in a cage, which expands deterministically and algebraically as t^α leading to $\beta_{\rm RW} = (1-2\alpha)$ for $\alpha < 1/2$ [43]. However, within this approach the exponent α has to be obtained from simulations. The fact that this methods gives the same result as the Lifshitz argument is a coincidence which follows from the Gaussian nature of the large y tail of the scaling function $G(y)$. Third, the Lifshitz approach does not only give the stretching exponent but also indicates the presence of the new length scale t^α with $\alpha = (2z+1)/4$, which gives the average distance between particles surrounding the surviving one. Furthermore, it shows that the fluctuations in the motion of these particles affect the stretching exponent. As the reduction of the DLCA to a three particle problem does not correctly take into account these fluctuations, the mean-field theory can not quantitatively describe the persistence in DLCA. Finally, the Lifshitz method is by no means rigorous and it would be worthwhile to try to analytically solve Eq. (13) with the appropriate boundary conditions. This would require ingenious analysis as the traditional image method [41, 1, 7] can not be applied.

The difference between the mean-field theory and the DLCA is evident also in the scaling of the interval size distribution between the particles (clusters) that surround a surviving particle (persistent cluster). The distribution for the random walk problem obeys a peculiar scaling [Eq. (16)] with a non-trivial length scale t^α but the corresponding distribution in the DLCA scales similarly to that of the cluster size distribution

$$P(l;t) = L^{-1} h\left(\frac{l}{L}\right), \tag{18}$$

where $L(t) \sim t^z$ is the average interval length between clusters. Although it is possible to estimate $h(x)$ from simulations, the Lifshitz argument can not be simply used to obtain the stretching exponent β_C. The outcome depends on the motion of the clusters next to the persistent ones. Therefore, the approach would require the knowledge of the distribution of their diffusion constants and also how they correlate with the distance from the persistent cluster.

3.2.4 Relation to Cluster Size Distribution

By definition, persistent clusters are those ones, which have not aggregated. Asymptotically these clusters belong to the small cluster size tail $s \ll S(t)$ of the cluster size distribution, which is characterized by the exponent τ or μ for $\gamma \geq 0$ or $\gamma < 0$, respectively. (See Section 1.4 for the definitions of these exponents). Therefore the exponents θ_C and β_C should relate to these. As all the exponents z, w, τ, μ, and θ_C are universal, it suffices to consider the simplest initial distribution, $n_s(0) = \delta_{s1}$. For $\gamma \geq 0$ the persistence exponent is given by $n_1(t) \sim t^{-\theta_C}$ but on the other hand $n_s(t) \sim t^{-w}$ for any fixed $s \geq 1$ [106]. Hence θ_C has to be equal to w and from Eq. (4) it follows that

$$\theta_C = (2 - \tau)z. \tag{19}$$

A similar argument for $\gamma < 0$ leads to

$$\beta_C = |\mu|z. \tag{20}$$

As μ follows directly from the scaling of the reaction kernel [29], the relation (20) makes cluster persistence for class III kernels a rather trivial quantity on a mean-field level. The same is true for class I kernels. However, in fluctuation dominated cases and for class II systems, as the one-dimensional DLCA, Eq. (19) (or Eq. (20)) can be used in the opposite direction: solving for the persistence one obtains the behavior of the small cluster size tail of the cluster size distribution, which is of primary importance in aggregation systems. As the reasoning leading to relations (19) and (20) is model independent, the behavior of the cluster size distribution may well be tackled through the concept of cluster persistence in other models, too. In fact, relations similar to (19) have been found in the reaction-diffusion system $A + A \to \emptyset$ [97, 98] and in the Ising model [58].

As $\theta_C = 2z$ for the one-dimensional DLCA when $\gamma > 0$, it follows from Eq. (19) that $\tau(\gamma) = 0$ for all $0 < \gamma < 2$. This independence of γ is surprising as the other exponents z and w depend on it. Here the explanation is again provided by the random walk picture: independent of γ (but $0 < \gamma < 2$) the motion of the persistent clusters becomes asymptotically irrelevant. Note that the polydispersity exponent is discontinuous at $\gamma = 0$ as $\tau(0) = 1$ [38]. Similar discontinuity is observed also in the Smoluchowski's rate equation theory for the sum kernel $K(i, j) = i^\lambda + j^\lambda$ in the limit $\lambda \to 0$ [107]. Here, similarly as for the persistence exponent, the determination of τ near $\gamma = 0$ by simulations is plagued by long lasting crossover effects, which led us to a wrong conclusion concerning the behavior of $\tau(\gamma)$ in Publication V. Figure 7b illustrates the scaling of the cluster size distribution in the γ-range, where the asymptotic regime can be reached.

We have concentrated here only on one-dimensional aggregation. As is evident from the above discussion, cluster persistence is an interesting quantity for the DLCA and also other aggregation systems in higher dimensions. There it should also be possible to find experimental realizations. On the other hand, in higher dimensions a similar mean-field random walk analysis is hardly possible (see, for example, [49]). We, however, believe that also for other systems the behavior of the cluster size distribution is determined by the solution of the cluster persistence problem.

4 Aggregation in an External Field

So far we have considered aggregation, in which the dynamics is purely diffusive. However, it is known that in colloidal suspensions the sedimentation of clusters due to gravitation becomes more pronounced as the growth proceeds. This alters both the growth mechanism and cluster structure as was recently observed in experiments [108] and simulations [71, 72].

In this Section we concentrate on the dynamic scaling in the presence of diffusion and drift. Both transport mechanisms are studied separately and simulation results are compared to the mean-field predictions in the case of one-dimensional cluster–cluster aggregation. With mixed dynamics the aggregation process leading to faster growth is shown to dominate the asymptotic dynamics, and a dynamic phase diagram characterizing the dominant growth mechanism is presented. Various crossovers are briefly discussed. This Section summarizes the results of Publication V.

4.1 Comparison of Simulations and Mean-Field Theory

The basis of the field–driven cluster–cluster aggregation model is the DLCA. In addition to the diffusive motion [$D(s) \sim s^{\gamma}$] clusters are also driven in one direction with a size dependent velocity $v(s) \sim s^{\delta}$, where δ is the field exponent. Figure 8a visualizes the dynamics when the drift dominates the large time aggregation behavior (compare to Fig 4). The mean-field Smoluchowski's rate equations described in Section 1.4 are directly applicable also to the field-driven case. Now the reaction kernel reads $K_v(i,j) \sim (i^{1/d_f} + j^{1/d_f})^{d-1}|i^{\delta} - j^{\delta}|$, and thus the driven system in d dimensions has similar scaling properties as the diffusive one in $d+1$ dimensions.

In one dimension the theory predicts, for example, that $z_{\mathrm{MF}} = 1/(1-\gamma)$ and $z_{\mathrm{MF}} = 1/(1-\delta)$ in the diffusive and driven cases, respectively. As shown in Publication V, simulations confirm the field-driven result whereas for the purely diffusive motion $z = 1/(2-\gamma)$ [109, 110]. The correct results can be simply understood by considering the characteristic length scales: the diffusive one $l_D \sim \sqrt{Dt}$ and the ballistic one $l_v \sim vt$. Assuming that the growth is asymptotically governed only by a single scale, it follows using $D(s) \sim s^{\gamma}$ and $v(s) \sim s^{\delta}$ that $z = 1/(2-\gamma)$ and $z = 1/(1-\delta)$ in the diffusion and field-driven cases, respectively. If both diffusion and

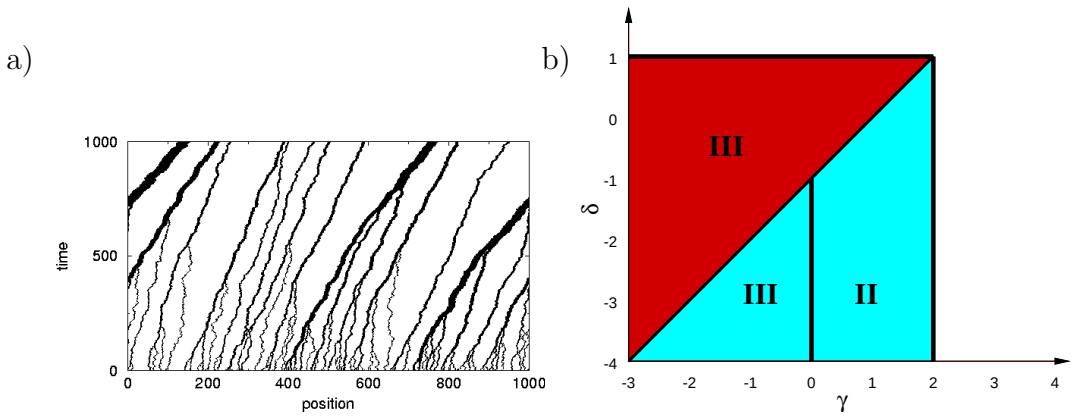

Figure 8: a) Space-time plot in the presence of mixed dynamics for $\gamma = -1.0$ and $\delta = 0.5$. b) The dynamic phase diagram. Aggregation is dominated by diffusion (light blue), drift (red) or a gelation transition (white). Roman numbers indicate the classes according to the decay of the small s tail of the cluster size distribution.

drift are present, the dynamics leading to faster growth dominates, i.e. $z = \max\{1/(2-\gamma), 1/(1-\delta)\}$. Hence, there is a crossover between the two behaviors at $\delta = \gamma - 1$. This leads to the dynamic phase diagram shown in Fig. 8b.

Consider next the scaling of the cluster size distribution, Eq. (3). The mean-field theory predicts that for a diffusion (field) dominated dynamics the scaling function should decay fast [$f(x) \sim \exp(-x^{-|\mu|})$; class III] for $\gamma < 0$ ($\delta < 0$) and as a power-law [$f(x) \sim x^{-\tau}$; class II] for $\gamma \geq 0$ ($\delta \geq 0$) at small argument values. Simulations confirm the change of the class for the diffusive case but not for the field-dominated one. The drift dominated aggregation always belongs to class III, where the large-small collisions dominate the aggregation. This is opposite to the predictions for the dynamic exponent, in which case the mean-field theory works better for the driven dynamics. Note, however, that if one replaces the mean-field value for z by the correct one in the DLCA, all the simulation results studied in Publication V are consistent with the mean-field predictions.

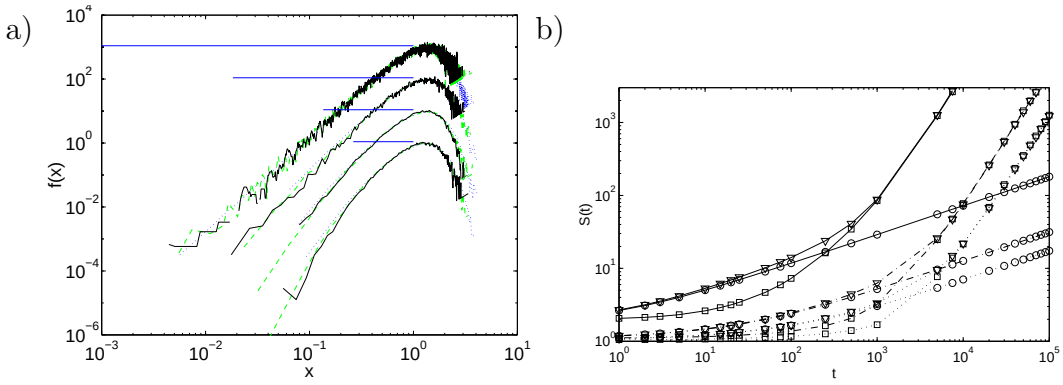

Figure 9: a) The scaling functions for the DLCA for $\gamma = -0.05$, -0.25, -0.50, and -0.75 (from top to bottom). Horizontal lines show the crossover region $\exp(1/\gamma) \leq x \leq 1$ where the scaling functions show typical class II behavior. The data for various γ-values have been shifted in the vertical direction to make the figure clearer. b) Average cluster size for $\gamma = -0.5$ and $\delta = 0.5$ in the diffusive ($\bigcirc$), driven ($\square$), and driven diffusive (∇) cases. Concentrations $\phi = 0.05$ ($\cdots$), 0.1 ($-\cdot$), and 0.5 (—).

4.2 Crossover Behaviors

There are three types of crossovers when the drift is included. Consider, as an example, the purely diffusive case. The first one was already discussed in the context of cluster persistence in Section 3.2 when $\gamma > 0$ but close to zero. In that region aggregation is characterized by the $\gamma = 0$ behavior for intermediate times and reaches the true asymptotic behavior only for $t^{\gamma z} \gg 1$. For example, for γ as large as 0.25 $t^{\gamma z} = 10$ corresponds to $t \approx 10^7$. The simulations reported in Article V do not reach large enough times and the analysis considering the dependence of the polydispersity exponent τ on γ is incorrect (the correct analysis leading to $\tau(0) = -1$ and $\tau(\gamma) = 0$ for $0 < \gamma < 2$ is presented in Articles III and IV and in Section 3.2).

The second crossover between class II and III behaviors takes place for $\gamma < 0$ but close to zero. Figure 9a shows the cluster size distributions using the scaling form of Eq. (3). The scaling function $f(x)$ shows typical class II type of behavior in the crossover region $\exp(1/\gamma) \ll s/S(t) \ll 1$. This agrees with the mean-field analysis [29]. In dimensions $d = 2$ and 3 the transition point between class III- and class II-behaviors has been argued to be at a negative γ [35]. However, crossover effects are not considered and the

analysis resorts to the fact that the cluster size distribution would change smoothly from a non-monotonic function to a monotonic one, i.e. $\tau = 0$ at the transition point. This is clearly incorrect for the one-dimensional DLCA, where the spatial fluctuations are stronger than in higher dimensions. Hence, it is likely that the transition is located at $\gamma = 0$ in all dimensions.

Finally, there is a crossover related to the change from diffusion dominated growth to the field dominated one. The average cluster size at the crossover can be estimated by comparing the pairing time, i.e. the time during which $S \to 2S$, due to the diffusion to that due to the drift. This leads to

$$S_{\mathrm{cross}} \approx \left(\frac{2D_1\phi}{Av_1r_0} \right)^{1/(\delta-\gamma+1)}, \tag{21}$$

where r_0 is the elementary particle radius, D_1 and v_1 are its diffusion and drift constants, respectively, and A is a constant of order one characterizing the width of the scaling function $f(x)$. The numerics agrees reasonably well with Eq. (21) (Fig. 9b).

5 Coarsening of Sand Ripples

Now we turn to a different type of growth, to the coarsening of sand ripples considered in Publication VI. The dynamic evolution of ripples is a complicated phenomenon as a granular medium is driven by a hydrodynamic flow [111]. Here simplified models are used. The first, deterministic and symmetric mass transfer model, was originally proposed as a description of vortex ripples in coastal waters [112] and has thereafter been considered both theoretically [113] and experimentally [114]. The second, stochastic and asymmetric model, was introduced for wind driven ripples and solved on a mean-field level [115]. Here these two models are generalized such that they become comparable. The main focus is on the mass transfer in the evolution of the pattern. The mass transfer function, which gives the rate at which a ripple gains mass from its neighbors, is taken to be algebraic.

Section 5.1 introduces the ripple models. Although the physics of sand ripple formation differs from that of cluster-cluster aggregation, the stochastic ripple model can be mapped to aggregation, and for algebraically growing mass transfer functions the two models obey similar universal scaling. In Section 5.2 methods familiar from zero range processes [73, 74, 75] are used to obtain the exact asymptotic mass distribution when the loss of a ripple from the system involves a rare fluctuation. The asymptotic state is characterized by a product measure and thus the mean-field assumption made in [115] becomes justified. The approach to the asymptotic state is discussed by considering the nearest neighbor time-correlation function, which decays universally but depends on the symmetry of the mass transfer. The case of frequent ripple extinctions is demonstrated to be more tricky in Section 5.3 although it can be described by a system of deterministic differential equations.

5.1 Modeling Ripple Formation

On a general level ripple formation involves transfer of mass between ripples. Here we concentrate on the role of the transfer in the evolution of a ripple pattern within a simple, one-dimensional model [112] and its stochastic counterpart. Consider the direction perpendicular to the ripples and imagine the surface profile along a two-dimensional cut (see Fig. 10). In this plane each ripple can be described by it size λ_i (i indexes the ripples) and

Figure 10: Experimental image of vortex ripples in a one-dimensional annular geometry [114]. The amplitude of the fluid oscillations is denoted by a. The line above the pattern shows a fit of triangles with a constant slope. Courtesy of K.H. Andersen.

the system becomes one-dimensional. The ripple "size" is here used as a general measure with no distinction between the linear size of a ripple and the mass it contains (see [112] for a discussion of the difference between these two alternatives).

During the dynamic evolution, the neighboring ripples exchange mass with each other. The main assumption of the model is that the mass transfer rate to a ripple i depends only on its size. In the context of the formation of vortex ripples in coastal waters this is motivated by the observation that the mass transfer to a ripple is affected mostly by a separation vortex which appears in the wake of it. For vortex ripples the mass transfer rate $\Gamma(\lambda)$ is known to be a non-monotonic function with a maximum near $\lambda = a$, where a is the amplitude of the fluid oscillations [112, 114]. In the case of wind driven coarsening a leading ripple is eroded with a rate inversely proportional to the size of the trailing one [115]. Here we consider algebraic mass transfer rates $\Gamma(\lambda) \sim \lambda^\gamma$, which for $\gamma < 0$ generalize the study [115] on wind ripple coarsening and for $\gamma > 0$ provide a first step toward understanding unstable coarsening taking place at initial stages in systems characterized by a non-monotonic mass transfer function.

The noisy version of the model is defined on a lattice and a ripple at site i is characterized by its mass m_i, which corresponds to the variable λ_i defined above but whose values are restricted to integers. Ripples exchange unit masses with their nearest neighbors stochastically at a rate $\Gamma(m) = m^\gamma$. The dynamics is either symmetric, in which case mass is exchanged with both neighbors, or asymmetric such that mass is obtained only from the right neighbor. When the size of a ripple reaches zero, the corresponding lattice site is eliminated from the system and its neighboring ripples become neighbors of each other. The corresponding noiseless version of the model

is described by the equations [112]

$$\frac{\mathrm{d}\lambda_i}{\mathrm{d}t} = \frac{1}{2}[-\Gamma(\lambda_{i-1}) + 2\Gamma(\lambda_i) - \Gamma(\lambda_{i+1})], \tag{22}$$

and

$$\frac{\mathrm{d}\lambda_i}{\mathrm{d}t} = -\Gamma(\lambda_{i-1}) + \Gamma(\lambda_i) \tag{23}$$

for symmetric and asymmetric mass transfer, respectively.

The stochastic lattice model is similar to zero range processes [73, 74, 75], urn models [76], exclusion processes [74, 77, 78], and cluster–cluster aggregation. The details of the connections between these models can be found in Article VI and we only comment upon the relation to aggregation. First, the ripple model is mapped to an exclusion process of particles of unit size along the lines of [80], and the distances between particles correspond to the sizes of ripples. A hop of a particle can be considered as moving a cluster of particles as a whole. In this way the ripple system further maps to cluster–cluster aggregation, where clusters move with algebraic rates that depend on the distances to the neighboring clusters. Although the ripples correspond to empty spaces between clusters and the properties of clusters themselves have no relevance for the ripple coarsening, the growth is rather similar to that of DLCA for $\gamma > 0$. However, for $\gamma < 0$ there is a drastic difference as compared to DLCA due to the repulsive interaction between the clusters in the ripple model. Size independent rates ($\gamma = 0$) are not considered here as for this special case the model can be mapped to the exactly solvable problem of coalescing random walkers [39, 7] as discussed in Publication VI.

5.2 Noise-Induced Coarsening ($\gamma < 0$)

For $\gamma < 0$ a homogeneous state of equally sized ripples, $\lambda_i = \bar{\lambda}$, is stationary and linearly stable under the evolution equations (22) and (23) [112]. Independent of the initial condition the system eventually reaches a state, which no more coarsens. However, in the stochastic model the coarsening is driven by fluctuations, which lead to indefinite growth of the mean ripple size $\langle m \rangle(t)$. As the ripples near extinction are those with the highest incoming mass rates, the loss of a ripple is a rare fluctuation when the mean ripple size is large. Hence, the timescale of ripple extinctions and the one

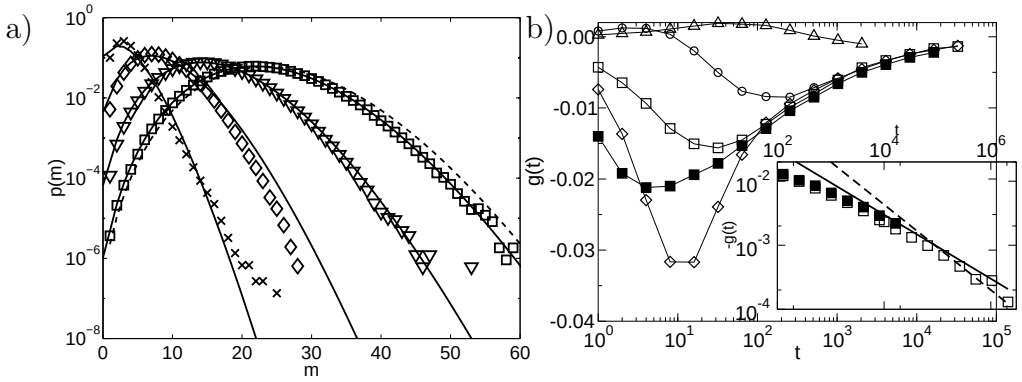

Figure 11: a) The ripple size distributions obtained from simulations for $\gamma = -0.5$ at $t = 4$ ($\times$), 128 ($\Diamond$), 4096 (∇), and 131072 ($\Box$) together with the analytical result (solid lines) [Eq. (24)] and its $\langle m \rangle \gg 1$ (dashed line) approximation for $t = 131072$. b) The nearest neighbor correlation function $g(t)$ for $\gamma = -1$. The initial condition is random ($\langle m \rangle(0) = 2$,$\Box$; $\langle m \rangle(0) = 1.2$,$\blacksquare$), monodisperse ($m(0) = 5$,$\Diamond$) or Poisson distributed ($\langle m \rangle(0) = 5$,$\bigcirc$; $\langle m \rangle(0) = 10$,$\Delta$). Open (filled) symbols correspond to asymmetric (symmetric) dynamics. The inset shows the decay at late times for the random case. The solid and dashed lines are guides to the eye with slopes $-1/2$ and $-2/3$, respectively.

at which the system would equilibrate itself in the absence of extinctions become well separated at late times.

In the absence of extinctions the steady state distribution can be shown to be given by a product measure. Utilizing methods familiar from zero range processes [75, 116], the probability of finding a ripple of size m is calculated exactly to be

$$p(m) = p_0 \alpha^m [(m-1)!]^\gamma, \tag{24}$$

where the constants p_0 and α are determined by the normalization condition $\sum_m p(m) = 1$ and the expectation value $\langle m \rangle = \sum_m m p(m)$. For example, for $\gamma = -1$ Eq. (24) is a shifted Poisson distribution and, in general, for $\langle m \rangle \gg 1$ it takes the form $p(m) = C_2(\gamma) e^{\gamma \langle m \rangle} \langle m \rangle^{-\gamma m - (1-\gamma)/2} [(m-1)!]^\gamma$. The analytical results are in an excellent agreement with the ones obtained from simulations (see Fig. 11a). Making the approximation that at long times the probability for a given ripple to vanish is equal to the probability $p(0)$ obtained by extrapolating the steady state probability distribution to

$m = 0$, results in a slow growth for the mean mass $\langle m \rangle(t) \approx -\ln(t)/\gamma$, to leading order in t. This is validated by simulations.

Due to the extinctions the product measure becomes exact only in the limit $t \to \infty$. To study the approach to the asymptotic distribution, the nearest neighbor time correlation function $g(t) = (\langle m_i m_{i+1} \rangle - \langle m \rangle^2)/\langle m \rangle^2$ is considered. The analysis is done in the continuum limit using hydrodynamic fluctuation theory for the coarse grained mass fluctuations in the quasi-steady state of mean mass $\langle m \rangle$. Concentrating on the long wavelength behavior the problem reduces to the behavior of the noisy Burgers equation [117], which has been widely studied in the context of driven diffusive systems [118, 119] and interface growth [120, 121, 122]. By inserting the parameters of the model to existing results [121, 122] gives, in the long time limit, the universal decays $g(t) \sim t^{-1/2}$ and $g(t) \sim t^{-2/3}$ for symmetric and asymmetric dynamics, respectively. The slow growth of the mean cluster size induces logarithmic corrections to the formulae given above. In both cases $g(t) < 0$ at late times and there will be anticorrelations between masses at neighboring sites. Simulations support the theoretical results although in the asymmetric case the asymptotic regime is preceded by a long crossover with a $t^{-1/2}$-decay (Fig. 11b).

5.3 Unstable Coarsening ($\gamma > 0$)

For $\gamma > 0$ the homogeneous state is linearly unstable [112]. The instability overcomes the noise, and the noisy and deterministic systems show asymptotically the same behavior. This is demonstrated in figure 12, which shows the scaling of the complement of the cumulative ripple size distribution $I(\lambda; t) = \int_\lambda^\infty \mathrm{d}x\, p(x; t)$ for $\gamma = 1$, where $p(x; t)$ is the number of ripples of size x at time t. According to the simulations the ripple size distributions are universal and for the linear mass transfer function ($\gamma = 1$) simple exponentials.

In Article VI a mean-field theory for the linear case $\gamma = 1$ is developed. It predicts that any initial distribution evolving under Eqs. (22) or (23) preserves its initial shape but gets scaled and shifted, in contrast to the simulations (see Fig. 12). The theory further predicts exponential growth for the mean cluster size with a rate, which depends on the initial ripple size distribution. Simulations show that it grows exponentially in a universal manner. Another mean-field theory based on rate equations similar to those

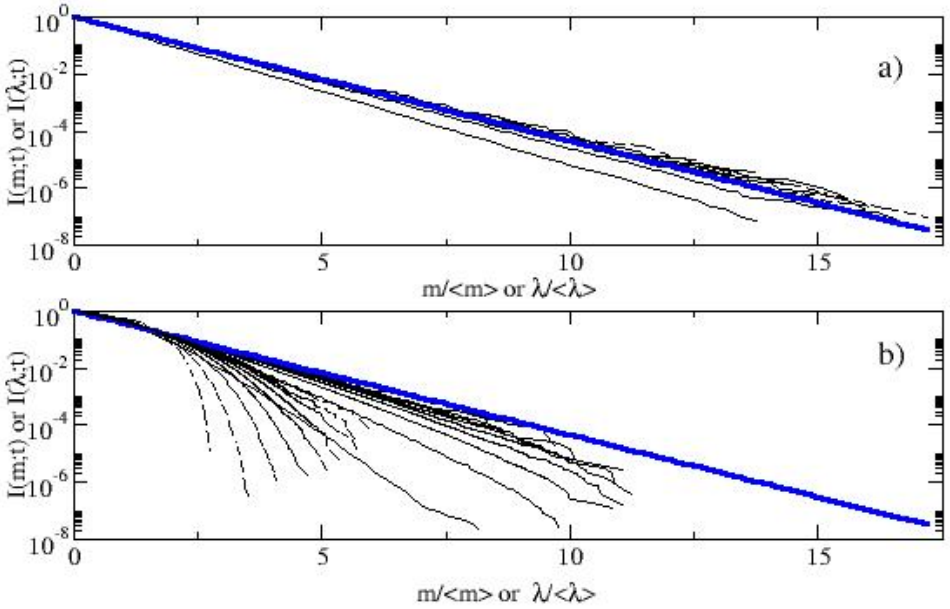

Figure 12: The complements of the cumulative ripple size distribution for $\gamma = 1$. a) The distributions for random (exponential) initial distribution with noisy (deterministic) dynamics are denoted by solid (dashed) lines. b) The distributions for monodisperse (flat) initial distribution with noisy (deterministic) dynamics are denoted by solid (dashed) lines. The curves are shown at times $t = 1, \ldots, 9$ and the thick solid lines in both figures represent the function $e^{-m/\langle m \rangle}$.

of Eq. (2) gives universal scaling [123, 81]. On the other hand, it fails in giving the numerically observed growth $\langle m \rangle(t) \sim t^{1/(1-\gamma)}$ for $0 < \gamma < 1$, which can be shown using simple scaling arguments. The failure of the mean-field theories is presumably due to the neglect of spatial fluctuations.

As is clear from the above discussion, the coarsening for $\gamma > 0$ is less well understood than for $\gamma \leq 0$ although it may be described by the deterministic system of equations (22) or (23). A better understanding of these would be desirable, especially in the case of a nonmonotonic mass transfer function, which has direct applications in the coarsening and the final ripple size selection of vortex ripples [112, 113, 114]. Finally, note the similarity with cluster-cluster aggregation for $\gamma \geq 0$: the cluster size distribution obeys dynamic scaling and the average cluster size grows algebraically.

6 Conclusions

This thesis consists of studies on nonequilibrium dynamics in various systems. First, diffusion through a random fiber network modeling paper is studied. A one-dimensional diffusion theory including fiber sorption is developed and demonstrated to be valid for diffusion of molecules through paper-like sheets of high enough thickness and porosity. The parameters of the theory are determined from fits to the numerically determined first-passage time distributions, which are calculated from random walk simulations in computer generated random fiber networks. An efficient simulation algorithm utilizing the planar geometry of the network and allowing for molecule-fiber interactions is presented. The estimated diffusion constants agree well with experimental measurements showing that gas diffusion through uncoated paper and board sheets can be efficiently simulated using model fiber networks, including the effects of fiber sorption.

Next, first-passage problems are considered in one-dimensional cluster-cluster aggregation when the diffusion constant of a cluster depends on its size as $D(s) \sim s^{\gamma}$. The emphasis is on the universal scaling of three persistences: the probabilities of a site to remain either empty or occupied and a cluster to remain unaggregated are studied. The filled site persistence is nonuniversal. The empty site persistence decays algebraically with an exponent twice as large as the dynamic exponent, which allows for a concise demonstration of the effect of two length scales on the scaling of the interval length distribution between persistent regions. Also the cluster persistence is universal and a mean-field theory based on three annihilating random walkers with time-dependent noise correlations is developed. When large cluster diffuse faster than small ones ($\gamma > 0$) the theory correctly describes the cluster persistence and the persistence exponent is, again, twice the dynamic one. The cluster persistence is connected to the behavior of the small size tail of the cluster size distribution, which in the present case is flat for $0 < \gamma < 2$. When small clusters diffuse faster than large ones ($\gamma < 0$), cluster persistence decays stretched exponentially but the mean-field theory gives only qualitative understanding. A Lifshitz tail argument shows that fluctuations remain relevant and indicates a new length scale in the random walk problem, which is related to distance between particles surrounding the surviving one.

If an external field, which drives clusters with a size dependent velocity $v(s) \sim s^{\delta}$, is present, the asymptotic dynamics in aggregation is dominated

by the process leading to the fastest growth. The dynamic phase diagram in the presence of mixed dynamics is presented with a phase boundary at $\delta = \gamma - 1$, in one dimension. The results are compared to a mean-field theory and various crossover effects are discussed. The one taking place near $\gamma = 0$ is shown to be relevant also for the cluster persistence.

Finally, one-dimensional stochastic and deterministic models are studied in the case of algebraic mass transfer rates $\Gamma(m) \sim m^\gamma$. The models are motivated by coarsening of sand ripples but they are connected to various nonequilibrium dynamical systems, which include zero-range processes, urn models, exclusion processes, and cluster-cluster aggregation. When mass is transferred preferably from large ripples to small ones ($\gamma < 0$), temporal correlations decay universally as $t^{-1/2}$ and $t^{-2/3}$ for symmetric and asymmetric mass transfer, respectively. Asymptotically the ripple size distribution is given by a product measure, which is calculated exactly. Ripple extinctions are rare events and the mean ripple size grows as $\langle m \rangle(t) \sim -\ln(t)/\gamma$. When small clusters vanish rapidly from the system ($\gamma > 0$), the noise in the dynamics is irrelevant but the mean-field theory developed fails to account for the numerically observed universality with respect to the initial ripple size distribution.

There are many interesting questions to be answered in the future. The most interesting is perhaps the effect of an external field on cluster structure, the study of which is in progress. Considering one-dimensional systems both the cluster persistence and the random walk survival problems present challenges for further analytical studies. From the practical point of view a deeper understanding of dynamic diffusion through thin sheets and the final ripple size selection in coarsening of vortex ripples are the most relevant. However, solving for these problems probably requires new theoretical methods to be developed.

References

[1] G. H. Weiss, *Aspects and Applications of the Random Walk*, 1st ed. (Elsevier Science, Amsterdam, 1994).

[2] J. W. Haus and K. W. Kehr, Phys. Rep. **150**, 263 (1987).

[3] A.-L. Barabási and H. E. Stanley, *Fractal Concepts in Surface Growth*, 1st ed. (Cambridge University Press, Cambridge, 1995).

[4] D. ben-Avraham and S. Havlin, *Diffusion and Reactions in Fractals and Disordered Systems*, 1st ed. (Cambridge University Press, Cambridge, 2000).

[5] *Nonequilibrium Statistical Mechanics in One Dimension*, 1st ed., edited by V. Privman (Cambridge University Press, Cambridge, 1997).

[6] N. Goldenfeld, *Lectures on Phase Transitions and the Renormalization Group*, fifth ed. (Addison–Wesley, Massachusetts, 1995).

[7] S. Redner, *A Guide to First-Passage Processes* (Cambridge University Press, New York, 2001).

[8] *Paper Physics*, 1st ed., edited by K. Niskanen (Fapet Oy, Helsinki, 1998).

[9] M. Deng and C. T. J. Dodson, *Paper: An Engineered Stochastic Structure*, 1st ed. (TAPPI Press, Atlanta, 1994).

[10] K. J. Niskanen and M. J. Alava, Phys. Rev. Lett. **73**, 3475 (1994).

[11] E. K. O. Hellén, M. J. Alava, and K. J. Niskanen, J. Appl. Phys. **81**, 6425 (1997).

[12] K. Niskanen, N. Nilsen, E. Hellén, and M. Alava, in *The Fundamentals of Papermaking Materials*, edited by C. F. Baker (Pira International, Leatherhead, 1997), pp. 1273–1292.

[13] A. Koponen, D. Kandhai, E. Hellén, M. Alava, A. Hoekstra, M. Kataja, and K. Niskanen, Phys. Rev. Lett. **80**, 716 (1998).

[14] H. Radhakrishnan, S. G. Chatterjee, and B. V. Ramarao, J. Pulp Paper Sci. **26**, 140 (2000).

[15] S. J. O'Donoghue and A. J. Bray, Phys. Rev. E **65**, 051114 (2002).

[16] P. Meakin, Phys. Rev. Lett. **51**, 1119 (1983).

[17] M. Kolb, R. Botet, and R. Jullien, Phys. Rev. Lett. **51**, 1123 (1983).

[18] P. Wiltzius, Phys. Rev. Lett. **58**, 710 (1987).

[19] P. Meakin, Z.-Y. Chen, and J. M. Deutch, J. Chem. Phys. **82**, 3786 (1985).

[20] G. M. Wang and C. M. Sorensen, Phys. Rev. E **60**, 3036 (1999).

[21] T. Sintes, R. Toral, and A. Chakrabarti, Phys. Rev. E **46**, 2039 (1992).

[22] P. Meakin, Phys. Scripta **46**, 295 (1992).

[23] P. Meakin, in *Phase Transitions and Critical Phenomena*, 1st ed., edited by C. Domb and J. L. Lebowitz (Academic Press, London, 1988), Vol. 12, Chap. 3, pp. 335–489.

[24] M. von Smoluchowski, Z. Phys. **17**, 585 (1916).

[25] K. Kang and S. Redner, Phys. Rev. A **30**, 2833 (1984).

[26] M. von Smoluchowski, Z. Phys. Chem. **92**, 129 (1917).

[27] R. M. Ziff, M. H. Ernst, and E. M. Henriks, J. Colloid Interface Sci. **100**, 220 (1984).

[28] R. M. Ziff, M. H. Ernst, and E. M. Hendriks, J. Phys. A **16**, 2293 (1983).

[29] P. G. J. van Dongen and M. H. Ernst, Phys. Rev. Lett. **54**, 1396 (1985).

[30] P. G. J. van Dongen and M. H. Ernst, J. Stat. Phys. **50**, 295 (1988).

[31] P. G. J. van Dongen, Phys. Rev. Lett. **63**, 1281 (1989).

[32] S. K. Friedlander, *Smoke, Dust, and Haze: Fundamentals of Aerosol Dynamics*, 2nd ed. (Oxford University Press, New York, 2000).

[33] R. Botet and R. Jullien, J. Phys. A **17**, 2517 (1984).

[34] S. Cueille and C. Sire, Phys. Rev. E **55**, 5465 (1997).

[35] P. Meakin, Phys. Rev. B **31**, 564 (1985).

[36] R. M. Ziff, E. D. McGrady, and P. Meakin, J. Chem. Phys. **82**, 5269 (1985).

[37] T. Vicsek and F. Family, Phys. Rev. Lett. **52**, 1669 (1984).

[38] J. L. Spouge, Phys. Rev. Lett. **60**, 871 (1988).

[39] D. ben-Avraham, in *Nonequilibrium Statistical Mechanics in One Dimension*, 1st ed., edited by V. Privman (Cambridge University Press, Cambridge, 1997), pp. 29–50.

[40] A. J. Bray and S. J. O'Donoghue, Phys. Rev. E **62**, 3366 (2000).

[41] M. E. Fisher, J. Stat. Phys. **34**, 667 (1984).

[42] M. E. Fisher and M. P. Gelfand, J. Stat. Phys. **53**, 175 (1988).

[43] P. L. Krapivsky and S. Redner, Am. J. Phys **64**, 546 (1996).

[44] M. Dronsker and S. R. S. Varadhan, Commun. Pure Appl. Math. **28**, 525 (1975).

[45] M. Dronsker and S. R. S. Varadhan, Commun. Pure Appl. Math. **32**, 721 (1979).

[46] M. Bramson and J. L. Lebowitz, Phys. Rev. Lett. **61**, 2397 (1988).

[47] P. Grassberger and W. Nadler, e-print, cond-mat/0010265.

[48] P. Grassberger, e-print, cond-mat/0201313.

[49] A. J. Bray and R. A. Blythe, e-print, cond-mat/0205381.

[50] S. N. Majumdar, Curr. Sci. (India) **77**, 370 (1999).

[51] S. N. Majumdar, C. Sire, A. J. Bray, and S. J. Cornell, Phys. Rev. Lett. **77**, 2867 (1996).

[52] B. Derrida, V. Hakim, and R. Zeitak, Phys. Rev. Lett. **77**, 2871 (1996).

[53] B. Derrida, A. J. Bray, and C. Godreche, J. Phys. A **27**, L357 (1994).

[54] D. Stauffer, J. Phys. A **27**, 5029 (1994).

[55] B. Derrida, V. Hakim, and V. Pasquier, Phys. Rev. Lett. **75**, 751 (1995).

[56] E. Ben-Naim and P. L. Krapivsky, J. Stat. Phys. **93**, 583 (1998).

[57] C. Sire and S. N. Majumdar, Phys. Rev. E **52**, 244 (1995).

[58] S. Jain and H. Flynn, J. Phys. A **33**, 8383 (2000).

[59] J. Krug, H. Kallabis, S. N. Majumdar, S. J. Cornell, A. J. Bray, and C. Sire, Phys. Rev. E **56**, 2702 (1997).

[60] H. Kallabis and J. Krug, Europhys. Lett. **45**, 20 (1999).

[61] S. N. Majumdar and A. J. Bray, Phys. Rev. Lett. **86**, 3700 (2001).

[62] Z. Toroczkai, T. J. Newman, and S. Das Sarma, Phys. Rev. E **60**, R1115 (1999).

[63] J. Farago, Europhys. Lett. **52**, 379 (2000).

[64] A. Dhar and S. N. Majumdar, Phys. Rev. E **59**, 6413 (1999).

[65] S. N. Majumdar and C. Sire, Phys. Rev. Lett. **77**, 1420 (1996).

[66] R. Buscall, Colloids Surfaces **43**, 33 (1990).

[67] S. R. Reddy, , D. H. Melik, and H. S. Fogler, J. Colloid Interface Sci. **82**, 116 (1981).

[68] H. Wang and R. H. Davis, J. Fluid Mech. **295**, 247 (1995).

[69] C. Allain, M. Cloitre, and M. Wafra, Phys. Rev. Lett. **74**, 1478 (1995).

[70] D. Senis and C. Allain, Phys. Rev. E **55**, 7797 (1997).

[71] A. E. González, Phys. Rev. Lett. **86**, 1243 (2001).

[72] A. E. González, J. Phys. Cond. Matter **14**, 2335 (2002).

[73] F. Spitzer, Adv. in Math. **5**, 246 (1970).

[74] H. Spohn, *Large Scale Dynamics of Interacting Particles* (Springer–Verlag, New York, 1991).

[75] M. R. Evans, Brazilian Journal of Physics **30**, 42 (2000), cond-mat/0007293.

[76] C. Godrèche and J. M. Luck, J. Phys. Cond. Matter **14**, 1601 (2002).

[77] T. M. Liggett, *Interacting Particle Systems* (Springer–Verlag, New York, 1985).

[78] B. Derrida and M. R. Evans, in *Nonequilibrium Statistical Mechanics in One Dimension*, 1st ed., edited by V. Privman (Cambridge University Press, Cambridge, 1997), pp. 277–304.

[79] S. N. Majumdar, S. Krishnamurthy, and M. Barma, Phys. Rev. Lett. **81**, 3691 (1998).

[80] S. N. Majumdar, S. Krishnamurthy, and M. Barma, J. Stat. Phys. **99**, 1 (2000).

[81] F. Leyvraz and S. Redner, Phys. Rev. Lett. **88**, 068301 (2002).

[82] B. Aurela and J. A. Ketoja, Food Additives and Contaminants **19**, 56 (2002).

[83] K. Binder and D. W. Heermann, *Monte Carlo Simulation in Statistical Physics*, 1st ed. (Springer–Verlag, Berlin, 1988).

[84] H. Gould and J. Tobochnik, *An Introduction to Computer Simulation Methods*, 1st ed. (Addison–Wesley, Massachusetts, 1996).

[85] S. Torquato, I. C. Kim, and D. Cule, J. Appl. Phys. **85**, 1560 (1999).

[86] S. Tolman and P. Meakin, Phys. Rev. A **40**, 428 (1989).

[87] H. Kaufman, A. Vespignani, B. B. Mandelbrot, , and L. Woog, Phys. Rev. E **52**, 5602 (1995).

[88] A. B. Harris, Y. Meir, and A. Aharony, Phys. Rev. B **36**, 8752 (1987).

[89] L. Nilsson, B. Wilhelmsson, and S. Stenström, Drying Techn. **11**, 1205 (1993).

[90] D. Stauffer and A. Aharony, *Introduction to Percolation Theory*, 2nd ed. (Taylor & Francis, London, 1994).

[91] J. A. Ketoja, B. Aurela, K. J. Niskanen, E. K. O. Hellén, and M. J. Alava, in *Proceedings of Barrier Coatings in Packaging Conference*, edited by M. Vähä-Nissi (Tampere University of Technology, Tampere, 2000).

[92] A. Bandyopadhyay, B. V. Ramarao, and S. Ramaswamy, Colloids Surf. A: Physicochem. Eng. Aspects **206**, 455 (2002).

[93] *Kinetics of Aggregation and Gelation*, edited by F. Family and D. P. Landau (North-Holland, Amsterdam, 1984).

[94] G. Manoj and P. Ray, e-print, cond-mat/9901130.

[95] E. Ben-Naim and P. L. Krapivsky, e-print, cond-mat/9902073.

[96] G. Manoj and P. Ray, e-print, cond-mat/9902339.

[97] G. Manoj and P. Ray, J. Phys. A **33**, L109 (2000).

[98] G. Manoj and P. Ray, J. Phys. A **33**, 5489 (2000).

[99] A. D. Rutenberg and B. P. Vollmayr-Lee, Phys. Rev. Lett. **83**, 3772 (1999).

[100] A. J. Bray, Phys. Rev. E **62**, 103 (2000).

[101] B. Derrida and R. Zeitak, Phys. Rev. E **54**, 2513 (1996).

[102] H. Risken, *The Fokker–Planck Equation*, 1st ed. (Springer–Verlag, Berlin, 1984).

[103] S. Redner and P. L. Krapivsky, Am. J. Phys **67**, 1277 (1999).

[104] L. Gálfi and Z. Rácz, Phys. Rev. A **38**, 3151 (1988).

[105] Z. Koza, Phys. A **240**, 622 (1997).

[106] P. G. J. van Dongen and M. H. Ernst, J. Phys. A **18**, 2779 (1985).

[107] P. G. J. van Dongen and M. H. Ernst, Phys. Rev. A **32**, 670 (1985).

[108] C. Allain, M. Cloitre, and F. Parisse, J. Colloid Interface Sci. **178**, 411 (1996).

[109] K. Kang, S. Redner, P. Meakin, and F. Leyvraz, Phys. Rev. A **33**, 1171 (1986).

[110] S. Miyazima, P. Meakin, and F. Family, Phys. Rev. A **36**, 1421 (1987).

[111] R. A. Bagnold, *The Physics of Blown Sand and Desert Dunes* (Chapman & Hall, London, 1941).

[112] K. H. Andersen, M.-L. Chabanol, and M. van Hecke, Phys. Rev. E **63**, 066308 (2001).

[113] J. Krug, Advances in Complex Systems **4**, 353 (2001).

[114] K. H. Andersen, M. Abel, J. Krug, C. Ellegaard, L. R. Søndergaard, and J. Udesen, Phys. Rev. Lett. **88**, 234302 (2002).

[115] B. T. Werner and D. T. Gillespie, Phys. Rev. Lett. **71**, 3230 (1993).

[116] V. Karimipour and B. H. Seradjeh, Europhys. Lett. **57**, 658 (2002).

[117] D. Forster, D. Nelson, and M. Stephen, Phys. Rev. A **16**, 732 (1977).

[118] H. van Beijeren, R. Kutner, and H. Spohn, Phys. Rev. Lett. **54**, 2026 (1985).

[119] B. Schmittmann and R. K. P. Zia, in *Phase Transitions and Critical Phenomena*, 1st ed., edited by C. Domb and J. L. Lebowitz (Academic Press, London, 1995), Vol. 17, pp. 1–220.

[120] M. Kardar, G. Parisi, and Y. Zhang, Phys. Rev. Lett. **56**, 889 (1986).

[121] J. Krug and H. Spohn, in *Solids Far From Equilibrium*, 1st ed., edited by C. Godrèche (Cambridge University Press, Cambridge, 1991), pp. 479–582.

[122] J. Krug, Adv. in Phys. **46**, 139 (1997).

[123] S. Ispolatov, P. Krapivsky, and S. Redner, Eur. Phys. J. B **2**, 267 (1998).